Cosmology from Non-Linear Weak Lensing

Zoltán Haiman

Andrea Petri, Jia Liu (Columbia)

Other collaborators:

Colin Hill (Columbia)
Morgan May (Brookhaven)
Lam Hui (Columbia)
Eugene Lim (Cambridge)
Xiuyuan Yang (Citibank)

Theory Seminar Univ. of Wisconsin, Madison 28 March 2017

Random Fields on the Sky

CMB

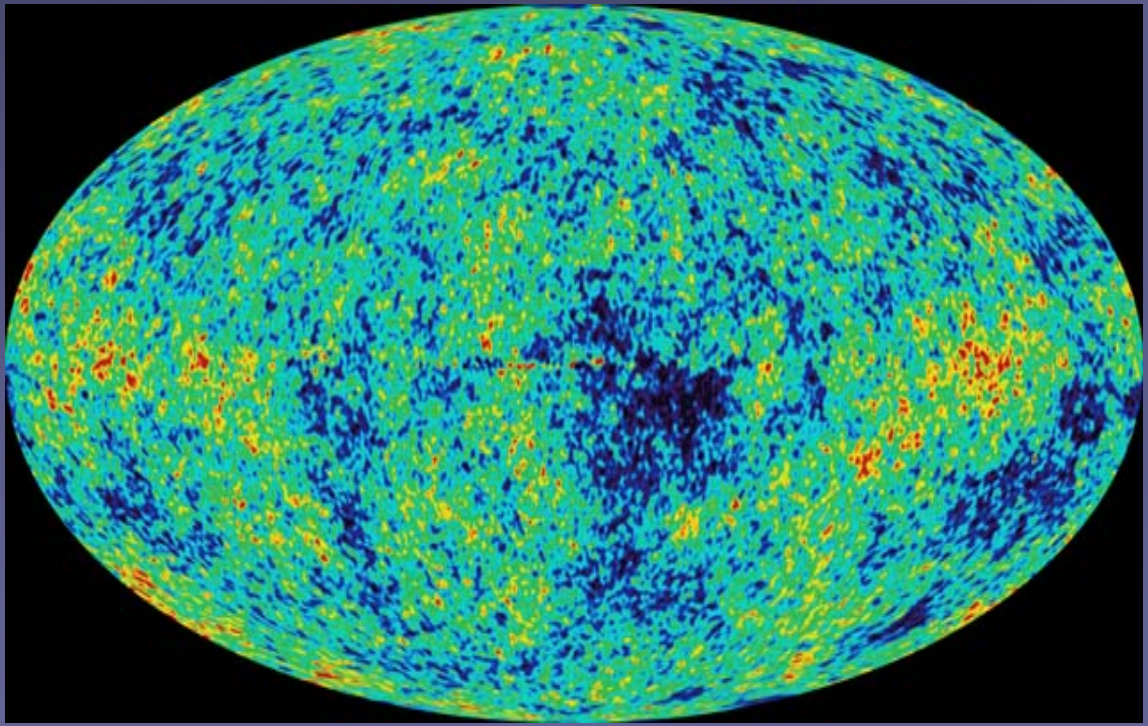

(almost) Gaussian

Lensing

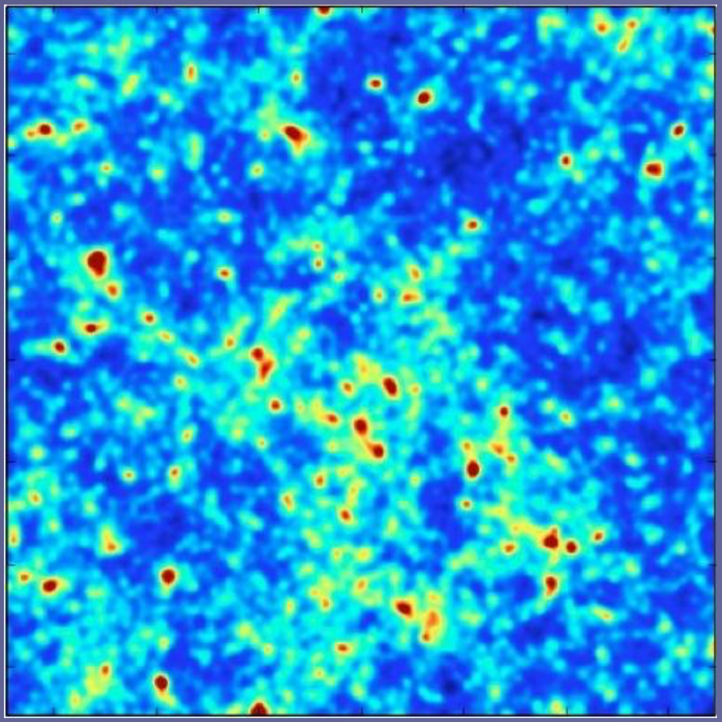

(very) non-Gaussian

Outline

- Overview of weak lensing and current results
- Lensing is not Gaussian!
- Cosmology with peak counts
- Application to CFHT data
- Alternative non-Gaussian statistics
- Systematic errors: theoretical + observational

The accelerating universe

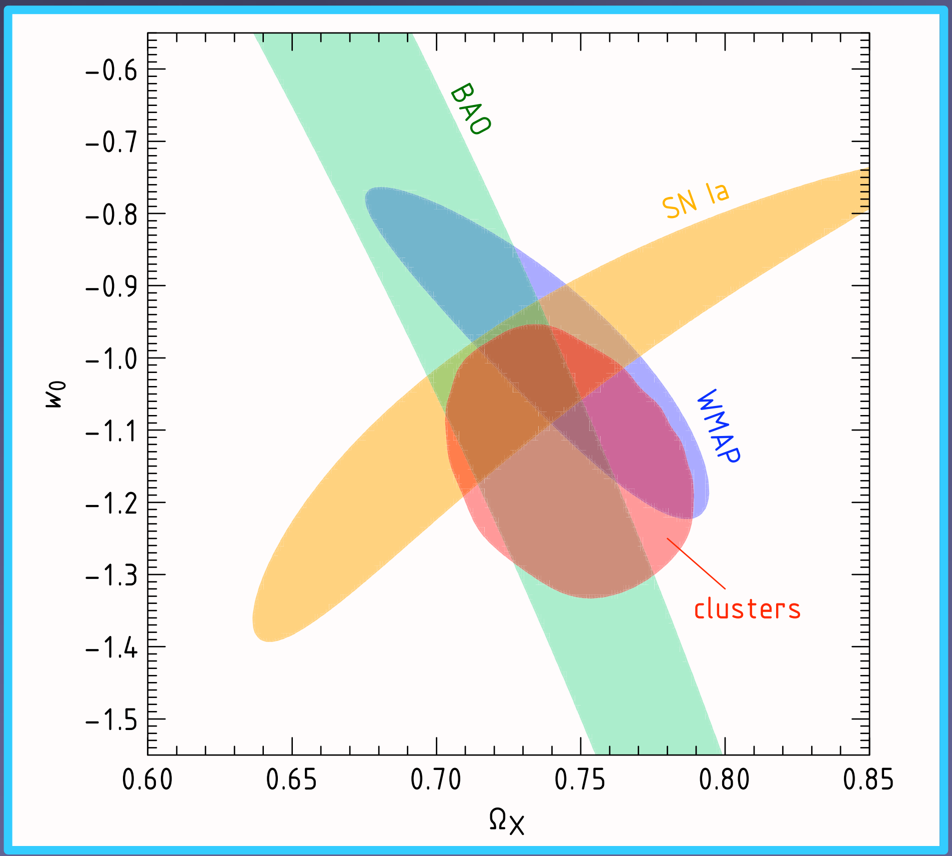

Vikhlinin et al. (2008)

Nature of **dark energy**:

1. vacuum energy density
2. dynamical field
3. modification to GR

Need, in the future:

- more **sensitivity** (esp. to w)
- combinations of experiments to **break degeneracies + systematics**
- especially useful to combine probes of **geometry & growth**

Cosmological Probes: Figures of Merit

Report of Dark Energy Task Force, Albrecht et al. (2006)

Baryon Acoustic Oscillations (BAO) (geometry)

Galaxy Clusters (CL) (geometry + growth)

Type Ia Sne (SN) (geometry)

Weak Lensing (WL) (geometry + growth)

Results for models

MODEL	$\sigma(w_0)$	$\sigma(w_a)$	$\sigma(\Omega_{DE})$	a_p	$\sigma(w_p)$	$[\sigma(w_a)\times\sigma(w_p)]^{-1}$
Stage II						
(CL-II+SN-II+WL-II)	0.115	0.523	0.01	0.79	0.04	53.82
BAO-IIIp-o	0.911	3.569	0.06	0.76	0.26	1.06
BAO-IIIp-p	1.257	5.759	0.06	0.79	0.32	0.55
BAO-IIIs-o	0.424	1.099	0.04	0.63	0.11	8.04
BAO-IIIs-p	0.442	1.169	0.04	0.64	0.12	6.97
BAO-IVLST-o	0.489	1.383	0.04	0.65	0.09	7.78
BAO-IVLST-p	0.582	1.642	0.05	0.65	0.13	4.58
BAO-IVSKA-o	0.202	0.556	0.02	0.64	0.03	55.15
BAO-IVSKA-p	0.293	0.849	0.02	0.66	0.05	21.53
BAO-IVS-o	0.243	0.608	0.02	0.61	0.04	42.19
BAO-IVS-p	0.330	0.849	0.03	0.62	0.06	19.84
CL-II	1.089	3.218	0.05	0.67	0.18	1.76
CL-IIIp-o	0.256	0.774	0.02	0.67	0.04	35.21
CL-IIIp-p	0.698	2.106	0.05	0.67	0.08	6.11
CL-IVS-o	0.241	0.730	0.02	0.67	0.04	38.72
CL-IVS-p	0.730	2.175	0.05	0.67	0.07	6.23
SN-II	0.159	1.142	0.03	0.90	0.11	7.68
SN-IIIp-o	0.092	0.872	0.03	0.95	0.08	13.91
SN-IIIp-p	0.185	1.329	0.03	0.89	0.12	6.31
SN-IIIs	0.105	0.880	0.03	0.94	0.09	12.39
SN-IVLST-o	0.076	0.661	0.03	0.95	0.07	22.19
SN-IVLST-p	0.150	1.230	0.03	0.91	0.10	7.93
SN-IVS-o	0.074	0.683	0.02	0.93	0.05	27.01
SN-IVS-p	0.088	0.692	0.03	0.94	0.08	19.10
WL-II	0.560	1.656	0.05	0.67	0.12	4.89
WL-IIIp-o	0.189	0.513	0.02	0.64	0.05	42.96
WL-IIIp-p	0.277	0.758	0.03	0.65	0.07	19.55
WL-IVLST-o	0.055	0.142	0.01	0.63	0.02	453.60
WL-IVLST-p	0.187	0.495	0.02	0.64	0.06	32.04
WL-IVSKA-o	0.039	0.118	0.00	0.68	0.01	645.76
WL-IVSKA-p	0.195	0.723	0.01	0.73	0.03	39.84
WL-IVS-o	0.063	0.169	0.01	0.64	0.02	310.10
WL-IVS-p	0.103	0.249	0.01	0.60	0.03	131.72

Gravitational Lensing

bending of light in general relativity

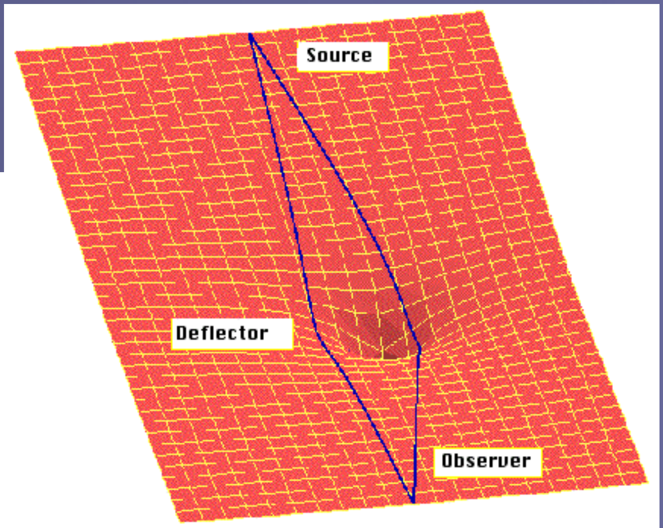

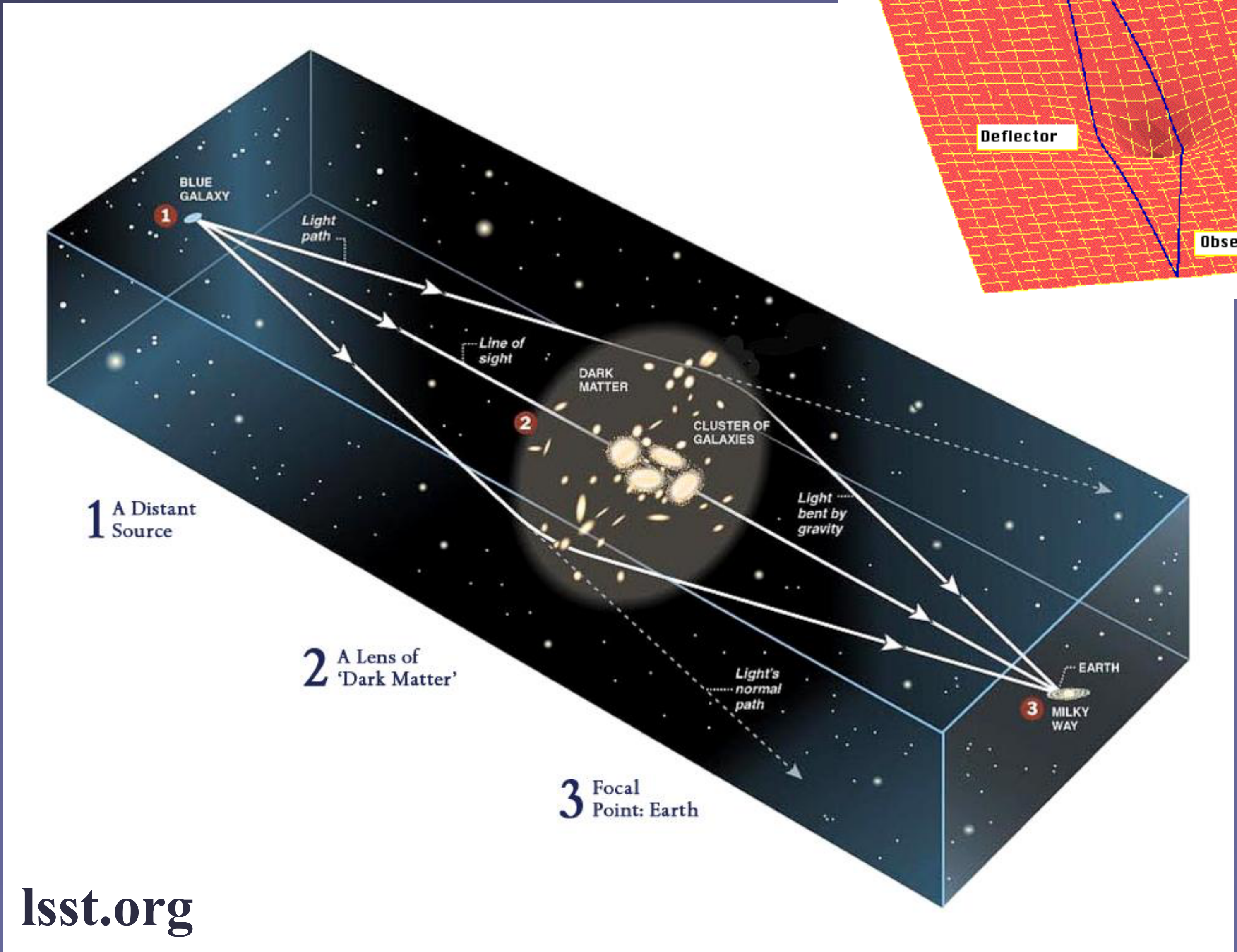

Gravitational Lensing by a Cluster

Abell 1689; Benitez et al. (2003)

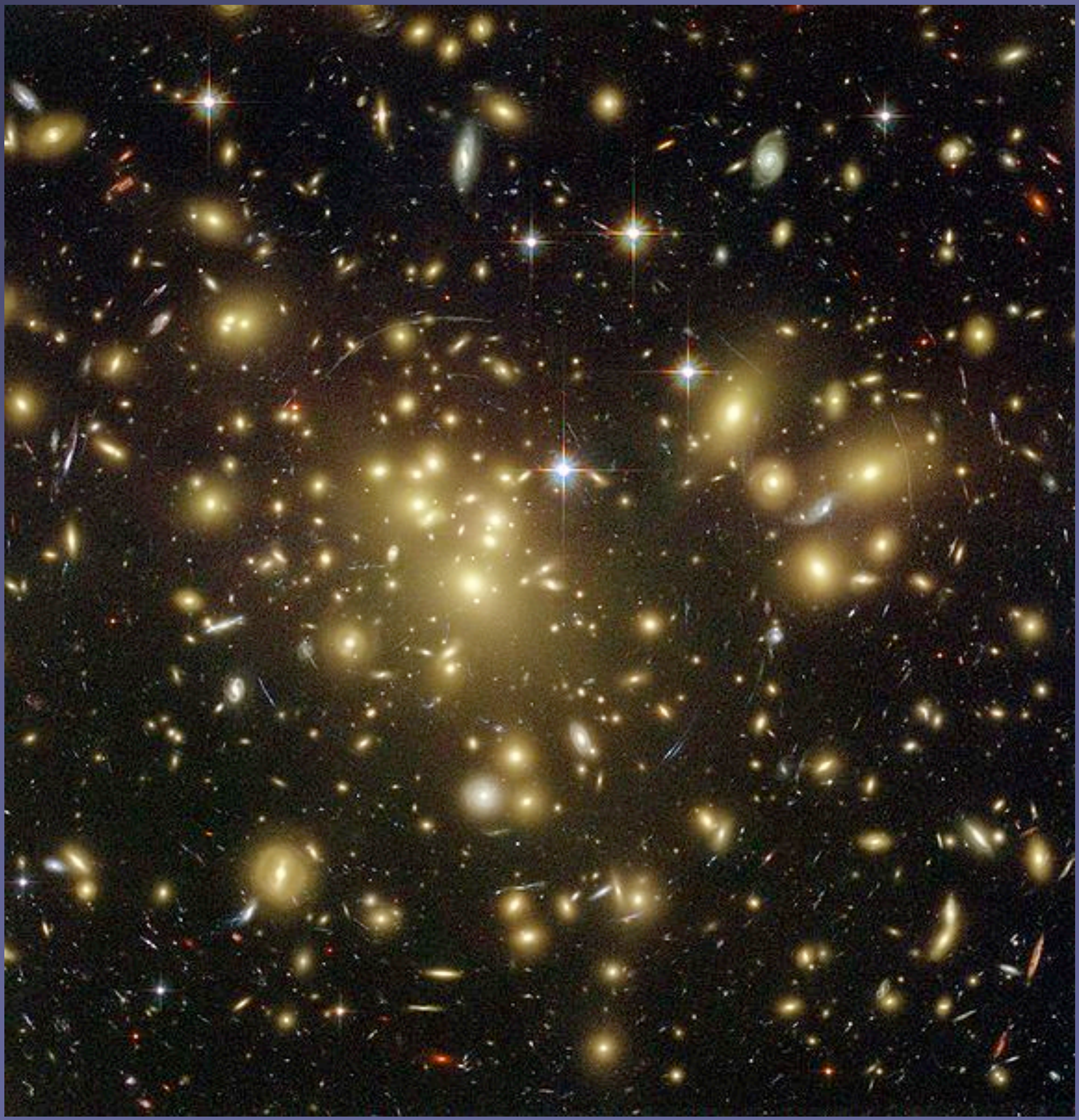

Cosmology with Weak Lensing

Distortion Tensor:

$$\psi_{ij} = 2\int_0^{\chi_s} d\chi\ \underbrace{(\chi_s - \chi)\frac{\chi}{\chi_s}}_{\text{lensing kernel}}\ \Phi_{,ij}(\vec{x}(\chi))$$

- Φ: gravitational potential.
- $\vec{x}(\chi)$: position of light ray at distance χ from observer.
- χ: distance from observer.
- χ_s: distance of source galaxy from observer.

$$\psi_{ij} \equiv \begin{pmatrix} -\kappa - \gamma_1 & -\gamma_2 \\ -\gamma_2 & -\kappa + \gamma_1 \end{pmatrix}$$

κ: convergence (magnification)

γ_1, γ_2: shear (distortion)

Kernel for source galaxy at distance $\chi_s = 3000$ Mpc:

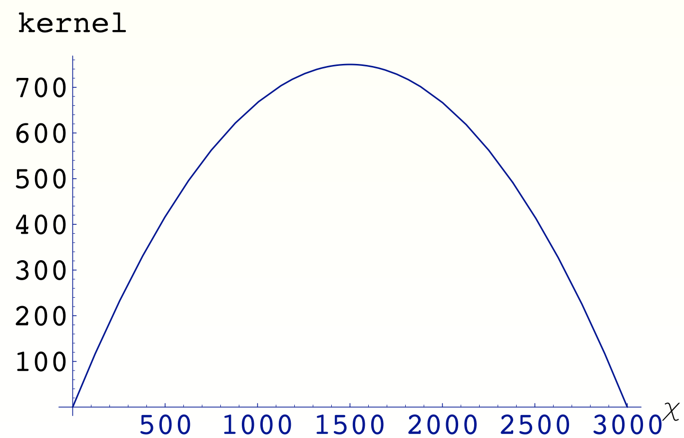

Cosmology with Weak Lensing

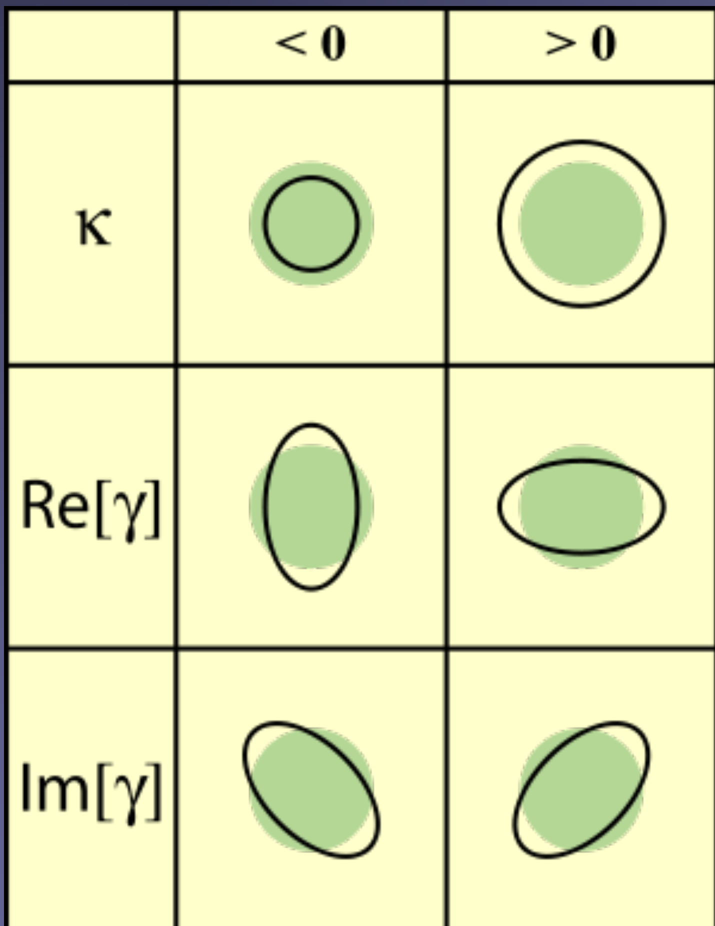

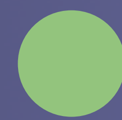

Source shape (θ_j)

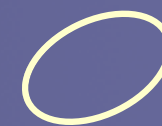

Observed shape (θ_i)

$$f_{obs}(\theta_i) = f_s(A_{ij}\theta_j)$$

$$A_{ij} = \begin{pmatrix} 1-\kappa-\gamma_1 & -\gamma_2 \\ -\gamma_2 & 1-\kappa+\gamma_1 \end{pmatrix}$$

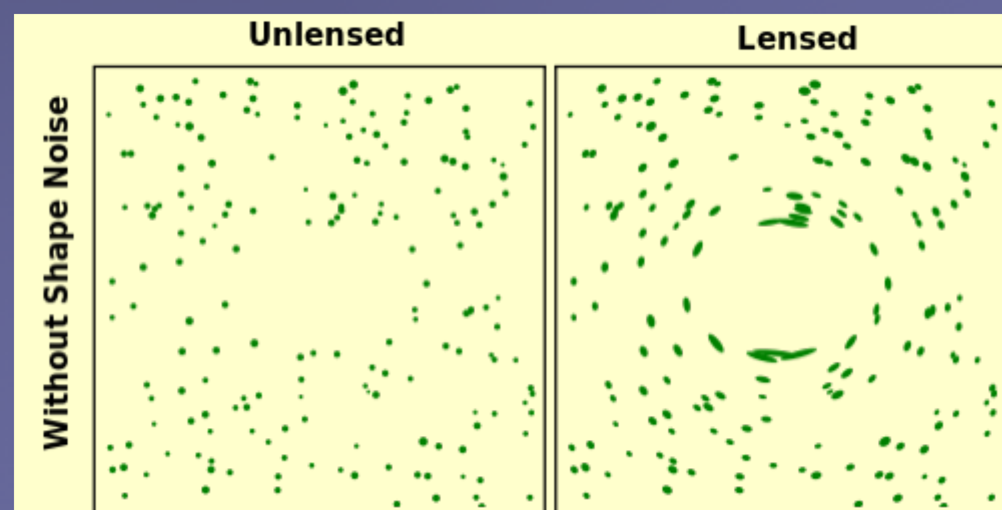

Wikipedia

Measuring Shear in Practice

Bridle et al. 2008

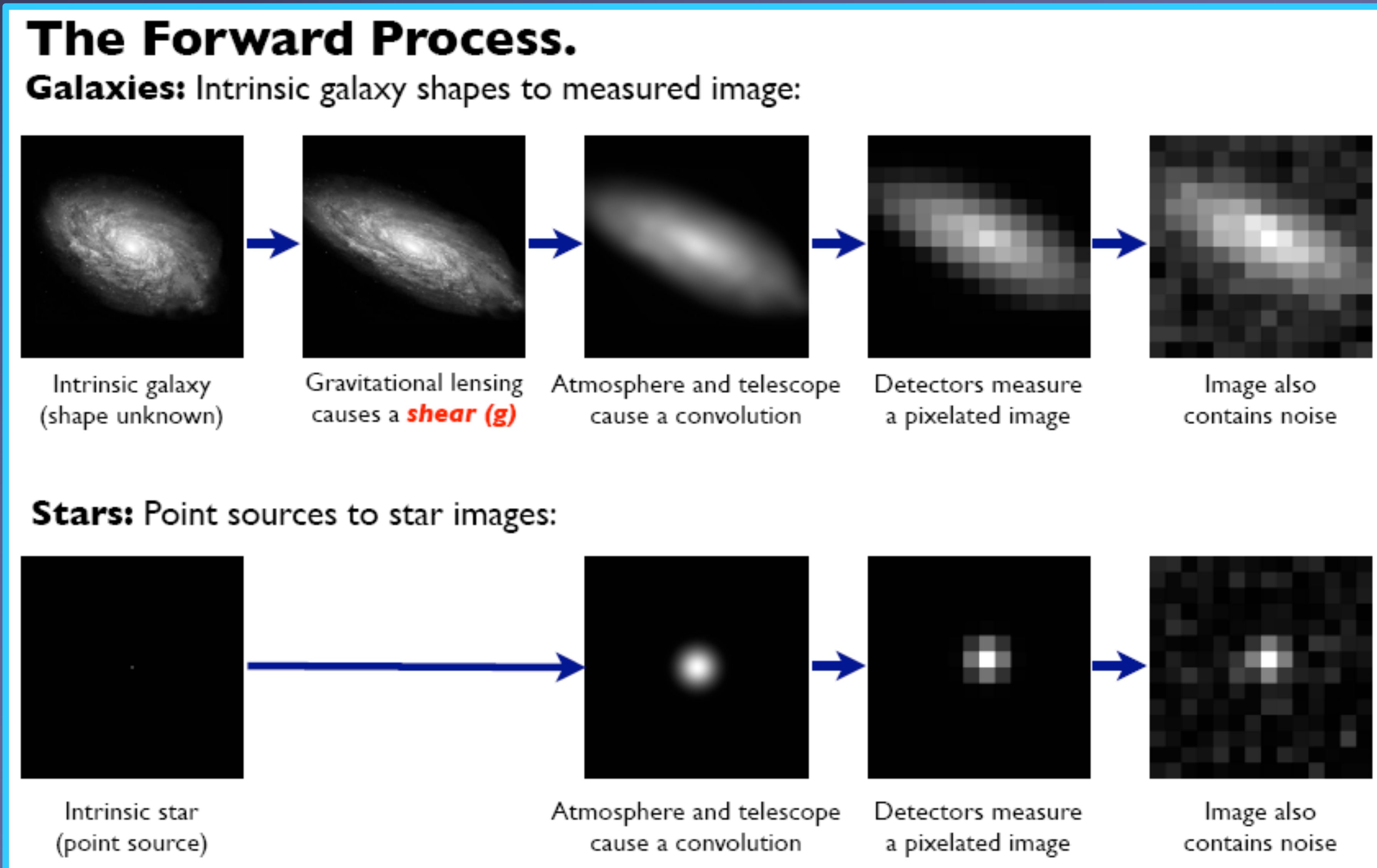

Weak Lensing by Large Scale Structure

"cosmic shear": random direction on the sky averages over l.o.s. fluctuations → O(1%)

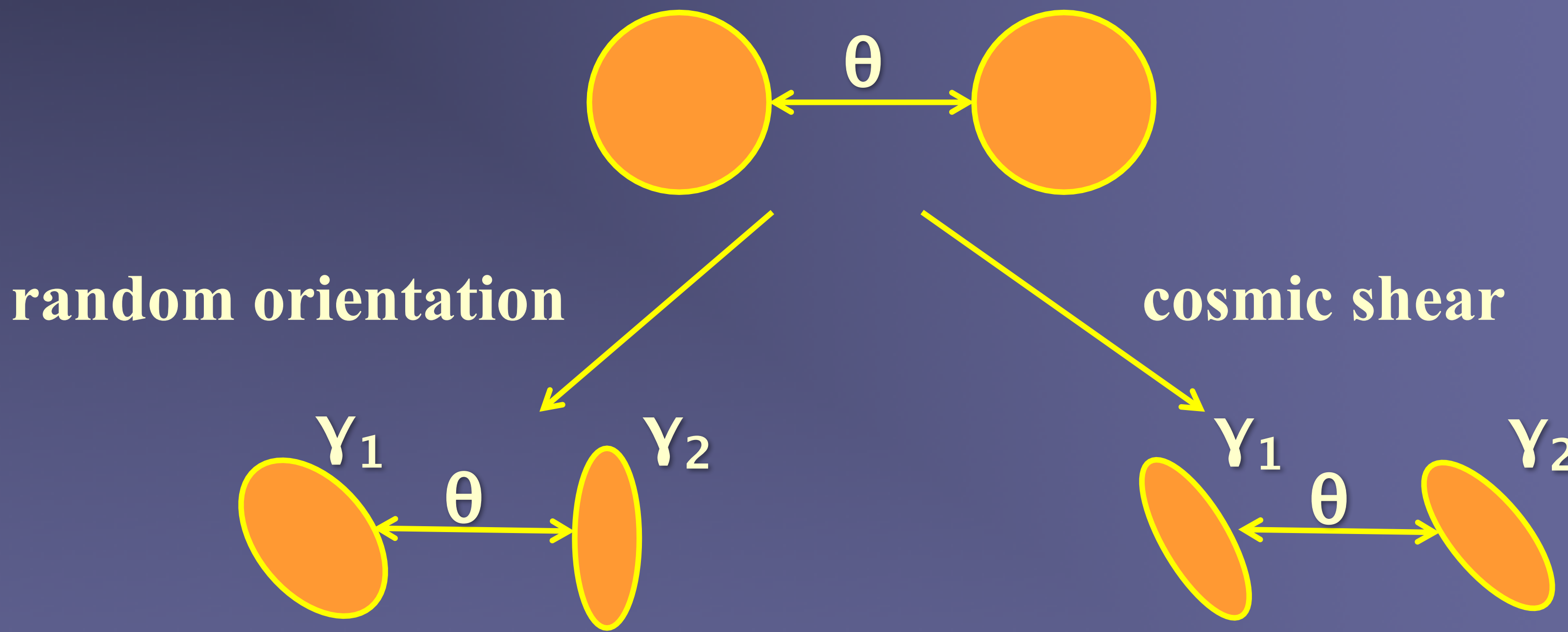

$C(\theta) = \langle \gamma_1 \gamma_2 \rangle = 0$

$C(\theta) = \langle \gamma_1 \gamma_2 \rangle \approx 10^{-4} \neq 0$

signal is weak, must average over many* galaxies

** = (0.2/√400) → 400 galaxies for S/N=1 detection of a systematic γ ~0.01*

→ $400 \times 10^4 = 4 \times 10^6$ galaxies for 1% error on γ ~0.01 → need ~100 deg²

Observable: convergence map

- Smoothing: average over ~ arcmin
- Tomography: bin galaxies by redshift

$$\hat{\kappa}(\mathbf{s}) = \frac{1}{2}\left(\frac{k_1^2 - k_2^2}{k_1^2 + k_2^2}\right)\hat{\gamma}_1(\mathbf{s}) + \frac{k_1 k_2}{k_1^2 + k_2^2}\hat{\gamma}_2(\mathbf{s})$$

Kaiser & Squires 1993

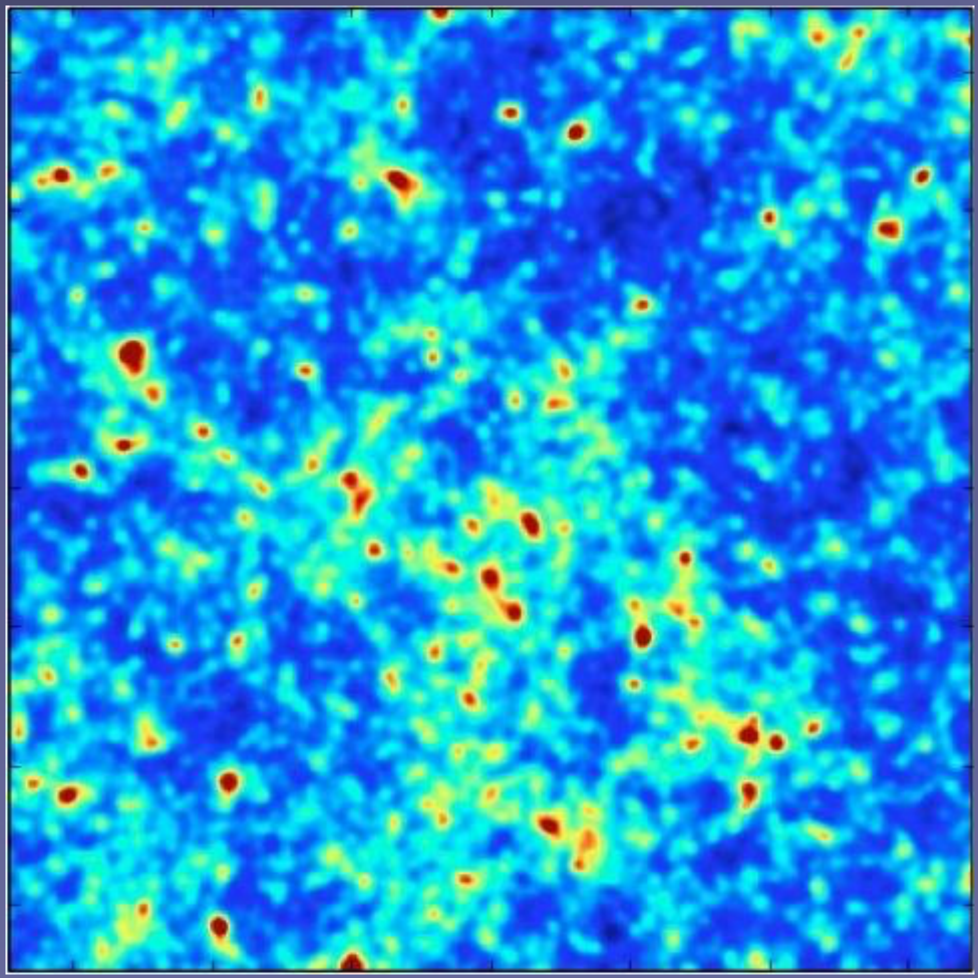

Weak Lensing: 2-point functions

- **Convergence power spectrum**

$$P_\kappa(l) = \frac{9}{4}\Omega_m^2 \frac{H_0^4}{c^4}\int_0^\infty dz \left[\frac{d\chi(z)}{dz}\right] \frac{\xi^2\left[\chi(z)\right]}{a^2(z)} P_{3\mathrm{D}}\left(\frac{l}{\chi(z)}; z\right),$$

$$\xi(\chi) = \int_z^\infty dz'\, n_{\mathrm{gal}}(z') \frac{\chi(z') - \chi(z)}{\chi(z')}.$$

- **Aperture mass statistic**

$$\left\langle \mathrm{M}_{\mathrm{ap}}^2 \right\rangle(\theta) = \frac{1}{2\pi}\int l\, dl\, P_\kappa(l)\, W(l\theta)^2.$$

Weak Lensing: 2-point functions

- **Convergence power spectrum**

$$P_\kappa(l) = \frac{9}{4}\Omega_m^2 \frac{H_0^4}{c^4}\int_0^\infty dz \boxed{\left[\frac{d\chi(z)}{dz}\right]} \frac{\xi^2[\chi(z)]}{a^2(z)} P_{3\mathrm{D}}\left(\frac{l}{\boxed{\chi(z)}};z\right),$$

$$\boxed{\xi(\chi)} = \int_z^\infty dz' \, n_{\mathrm{gal}}(z') \, \frac{\chi(z') - \chi(z)}{\chi(z')}.$$

- **Aperture mass statistic**

$$\langle \mathrm{M}_{\mathrm{ap}}^2 \rangle(\theta) = \frac{1}{2\pi}\int l \, dl \, P_\kappa(l) \, W(l\theta)^2.$$

Weak Lensing: 2-point functions

- **Convergence power spectrum**

$$P_\kappa(l) = \frac{9}{4}\boxed{\Omega_m^2}\frac{H_0^4}{c^4}\int_0^\infty dz\ \boxed{\left[\frac{d\chi(z)}{dz}\right]}\ \frac{\xi^2\left[\chi(z)\right]}{a^2(z)}\boxed{P_{3D}}\left(\frac{l}{\boxed{\chi(z)}};z\right),$$

$$\boxed{\xi(\chi)} = \int_z^\infty dz'\ n_{\mathrm{gal}}(z')\ \frac{\chi(z')-\chi(z)}{\chi(z')}.$$

- **Aperture mass statistic**

$$\left\langle \mathrm{M}_{\mathrm{ap}}^2 \right\rangle(\theta) = \frac{1}{2\pi}\int l\ dl\ P_\kappa(l)\ W(l\theta)^2.$$

Cosmology: Cosmic Shear

Schrabback et al. (2010)

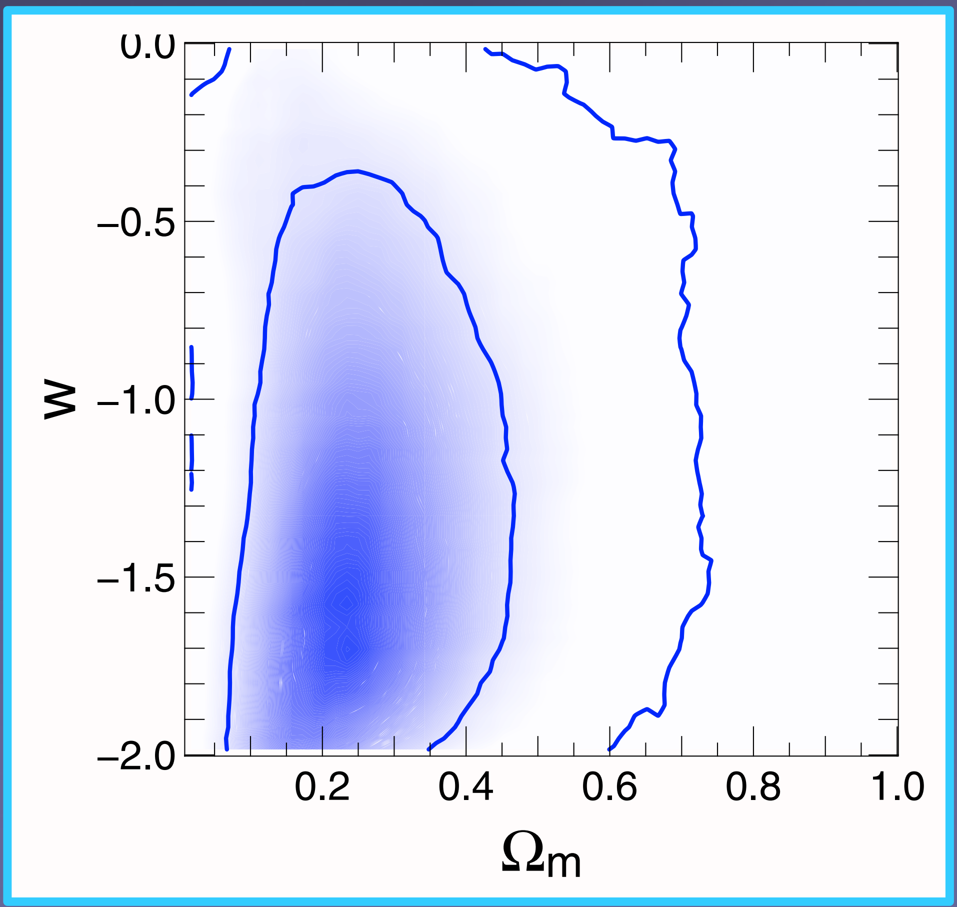

COSMOS survey

1.64 deg^2 of deep imaging with the Advanced Camera For Surveys (ACS) on HST

power spectrum tomography 450,000 galaxies in 5 z-bins, <z>~1.3, tail out to z>2

2σ detection of dark energy, independent of other probes

Also helps in combination with CMB, SN

Cosmology: Cosmic Shear

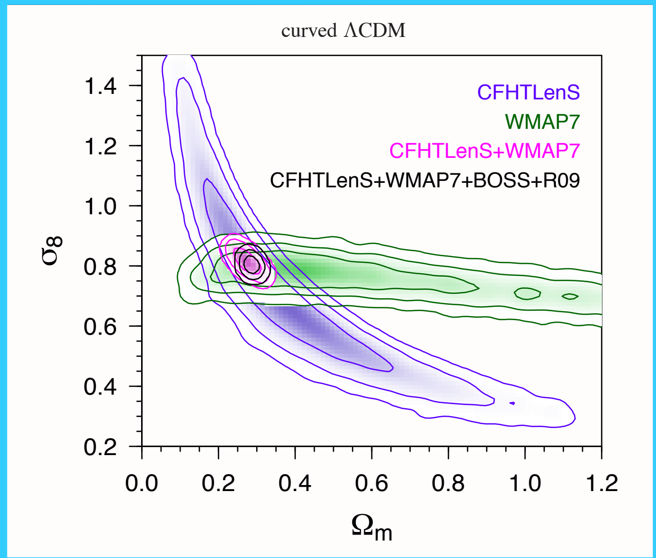

CFHTLenS survey

154 deg^2 of deep imaging with 3.6m CFHT - ~6×10^6 galaxies

2D - Kilbinger al. (2013)

single z-bin

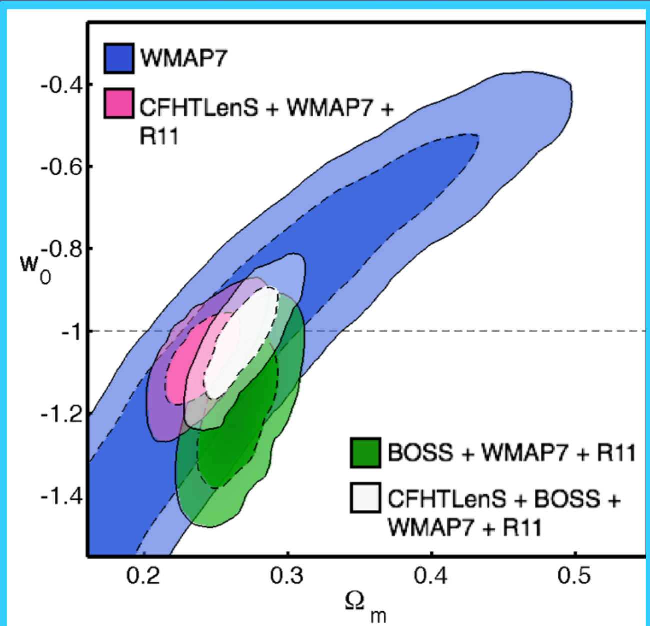

"3D" - Heymans al. (2013)

tomography in 6 z-bins, 0.2 < z < 1.3, with <z>~0.75 (includes IA model)

Outline

- Overview of weak lensing and current results
- Lensing is not Gaussian!
- Cosmology with peak counts
- Application to CFHT data
- Alternative non-Gaussian statistics
- Systematic errors: theoretical + observational

A 2D Gaussian Random Field

- CMB: goal is to look for *tiny* non-Gaussianity
- we can borrow some tools and apply to WL

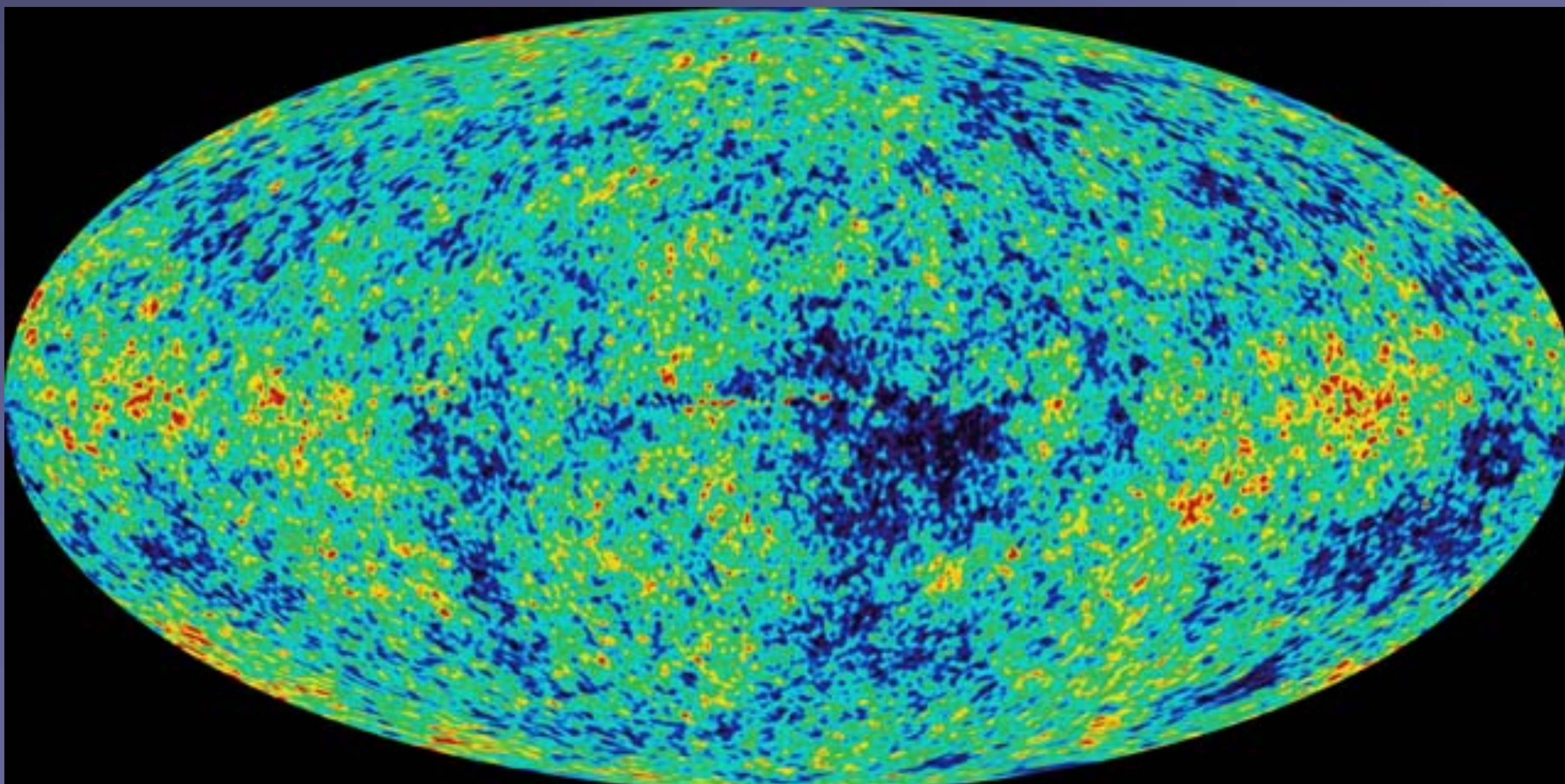

Cosmic Shear is Not Gaussian

Millennium simulation – Volker Springel, MPA

Cosmic Shear is Not Gaussian

- WL probes full projected overdensity field, including $\delta>1$
- one-point function of convergence: skewness, kurtosis, …

Fact: WL datasets contain large non-Gaussian features

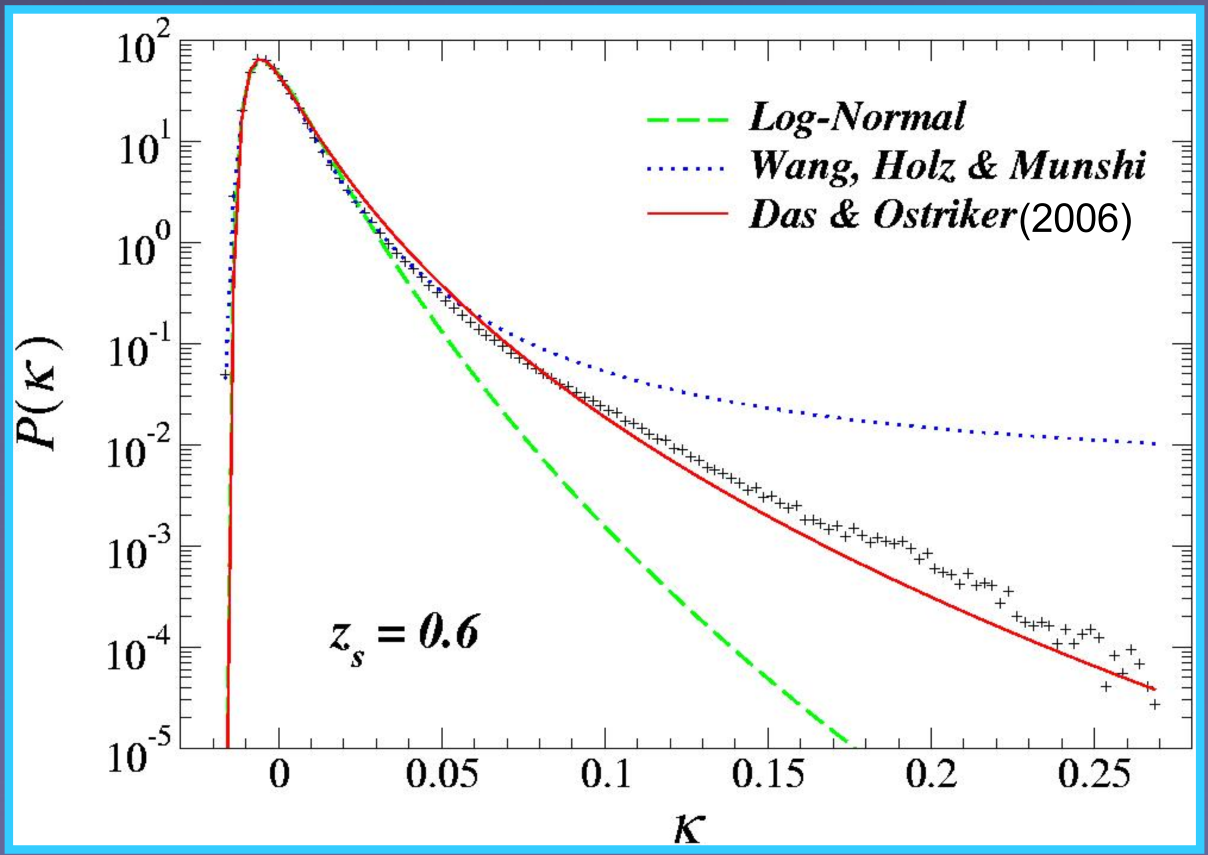

$F=\int_{\nu\sigma} P(\kappa)d\kappa$

Wang, Haiman & May (2009)

Cosmic Shear: 3-point function

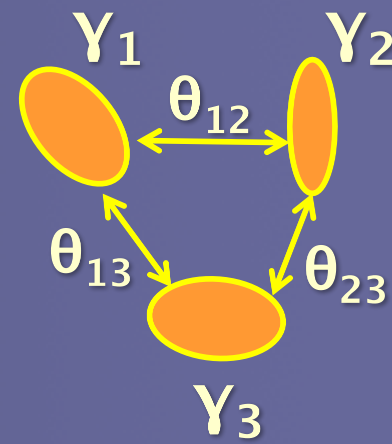

three-point shear statistics: $C(\theta_{12},\theta_{13},\theta_{23}) = \langle\gamma_1\gamma_2\gamma_2\rangle$
more difficult to predict and to measure

* $\langle M^3_{ap}\rangle(\Theta_1\Theta_2\Theta_3)$ can help tighten errors by ~10-20%
  Semboloni et al. (2011)
* small field not ideal Vafaei et al. (2010)

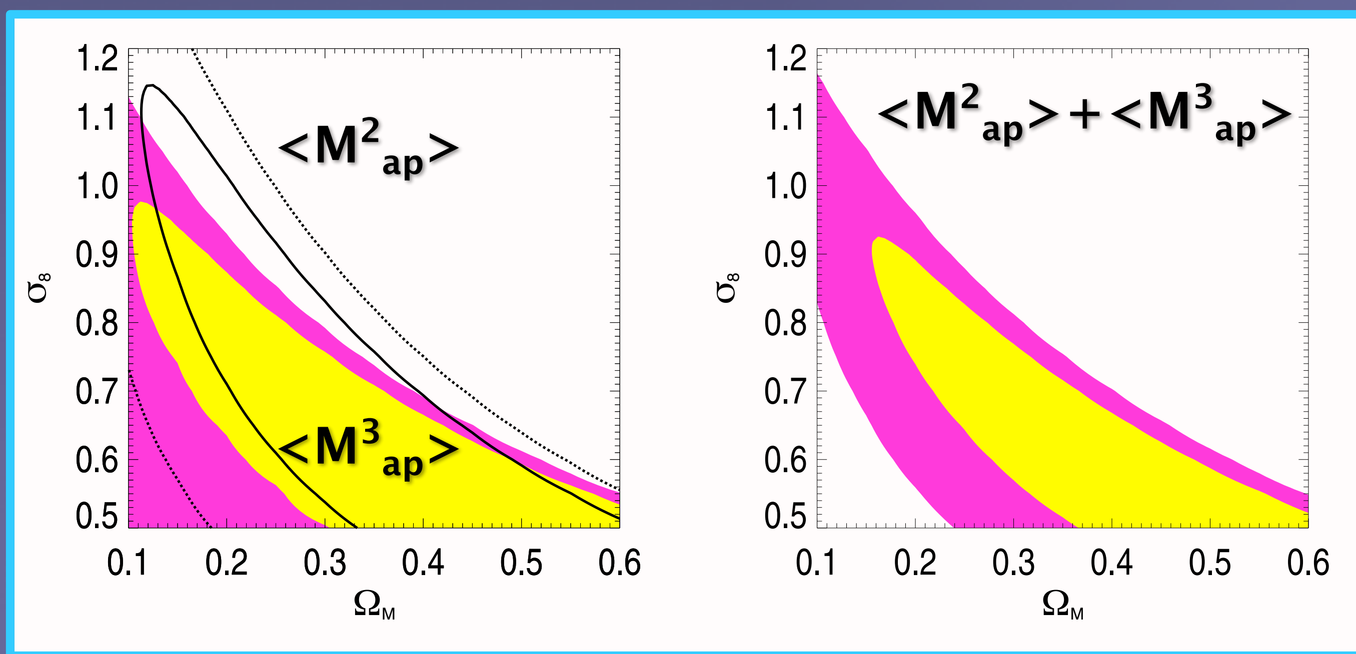

Skewness + Kurtosis Measurements

Van Waerbeke al. (2013)

CFHTLenS survey: 3.4m CFHT 154 $\deg^2$ 6×10^6 galaxies Kilbinger et al. (2013)

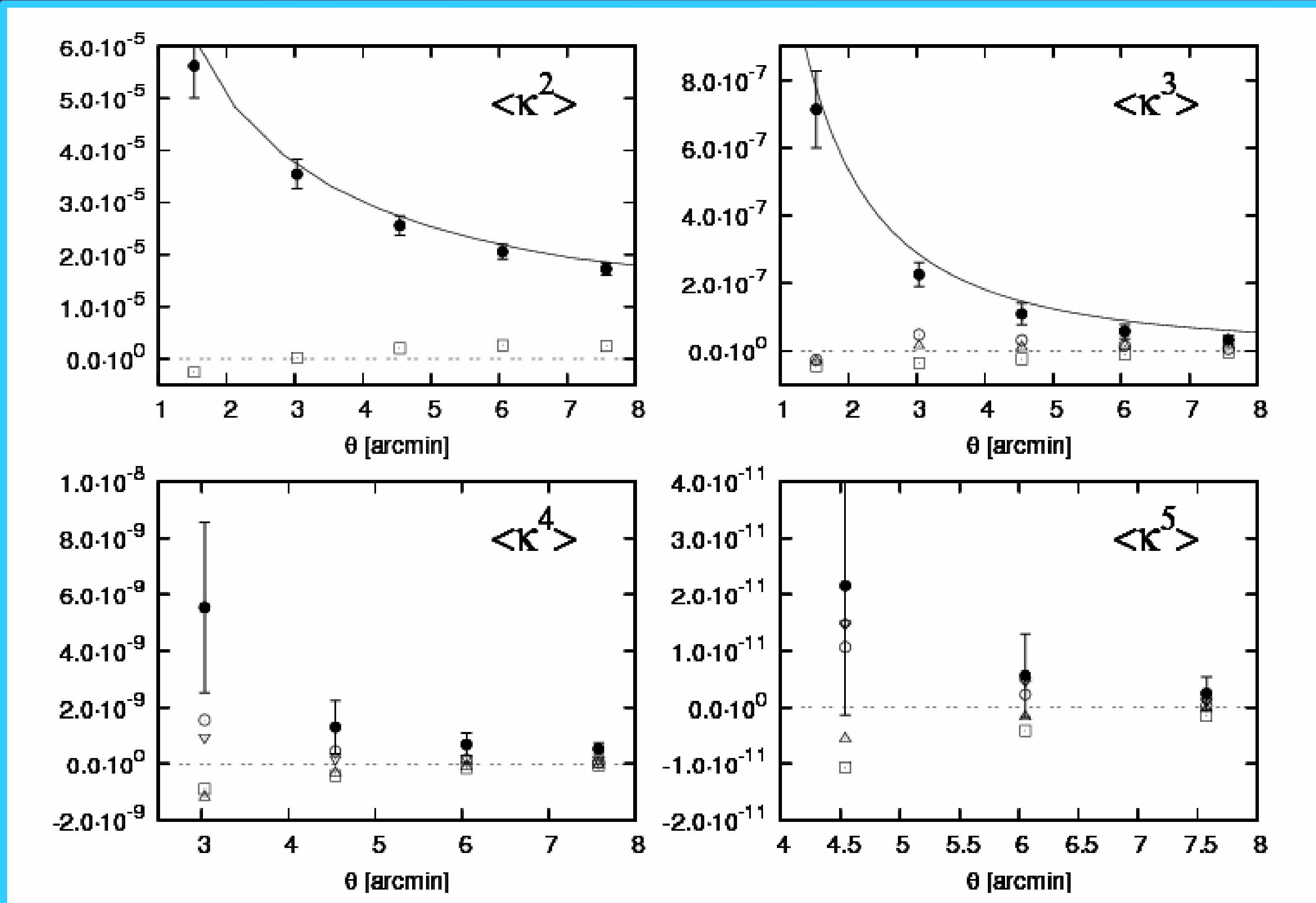

Outline

- Overview of weak lensing and current results
- Lensing is not Gaussian!
- Cosmology with peak counts
- Application to CFHT data
- Alternative non-Gaussian statistics
- Systematic errors: theoretical + observational

Peak counts

- A simple statistic: # of convergence peaks, regardless of whether or not they correspond to true bound objects

  as a function of *height*, *redshift* and *angular size*

  Kratochvil, Haiman, Hui & May (2010), PRD

  Yang, Kratochvil, Wang, Lim, Haiman & May (2011), PRD

  [Jain & van Waerbeke 2000 Marian et al. 2011, 2012, 2013; Maturi et al. 2010]

- Fundamental questions about "false" (non-cluster) peaks:

  1. How does N_{peak} depend on cosmology ?
  2. What is the field-to-field variance ΔN_{peak} (or C^{ij}_{peak})?

- Requires simulations

  (N_{peak} predictable in GRF: Bond & Efstathiou 1987)

N-body Simulations

- pure DM (no baryons, neutrinos, or radiation)
- public code GADGET-2, modified to handle $w_0 \neq -1$
- fiducial ΛCDM concodace cosmology :
  $(w_0, \Omega_\Lambda, \Omega_m, H_0, \sigma_8, n) = (-1.0, 0.74, 0.26, 0.72, 0.8, 1.0)$
- 512^3 box, size $200h^{-1}$ Mpc, z_{in}=60, $M_{DM}=4.3\times10^9\, M_\odot$
- gravitational softening length $\varepsilon_{Pl} = 7.5h^{-1}$ kpc
- output particle positions every $70h^{-1}$ comoving Mpc
- project mass onto 2D lens planes
- runs at NSF XSEDE Stampede

Mock Lensing Maps

- Ray-tracing

  - compute 2D potential (4096$\times$4096) in each lens plane
  - implement algorithm to follow rays (Hamana & Mellier 2001)
  - compute shear (γ), convergence (κ) and reduced shear (μ)

- Produce maps ('mock observations')

  - produce simulated 3.5$\times$3.5 deg^2 maps
  - raytrace towards the 2048$\times$2048 pixels
  - add noise: rotate each galaxy by random angle
  - reconstruct 2D κ-map from γ (Kaiser & Squires 1993)
  - smooth κ-map with 2D finite Gaussian 0.5 - 10 arcmin
  - repeat 1,000 times

- Identifying peaks

  - find all local maxima, record their height κ_{peak}

Peak Counts

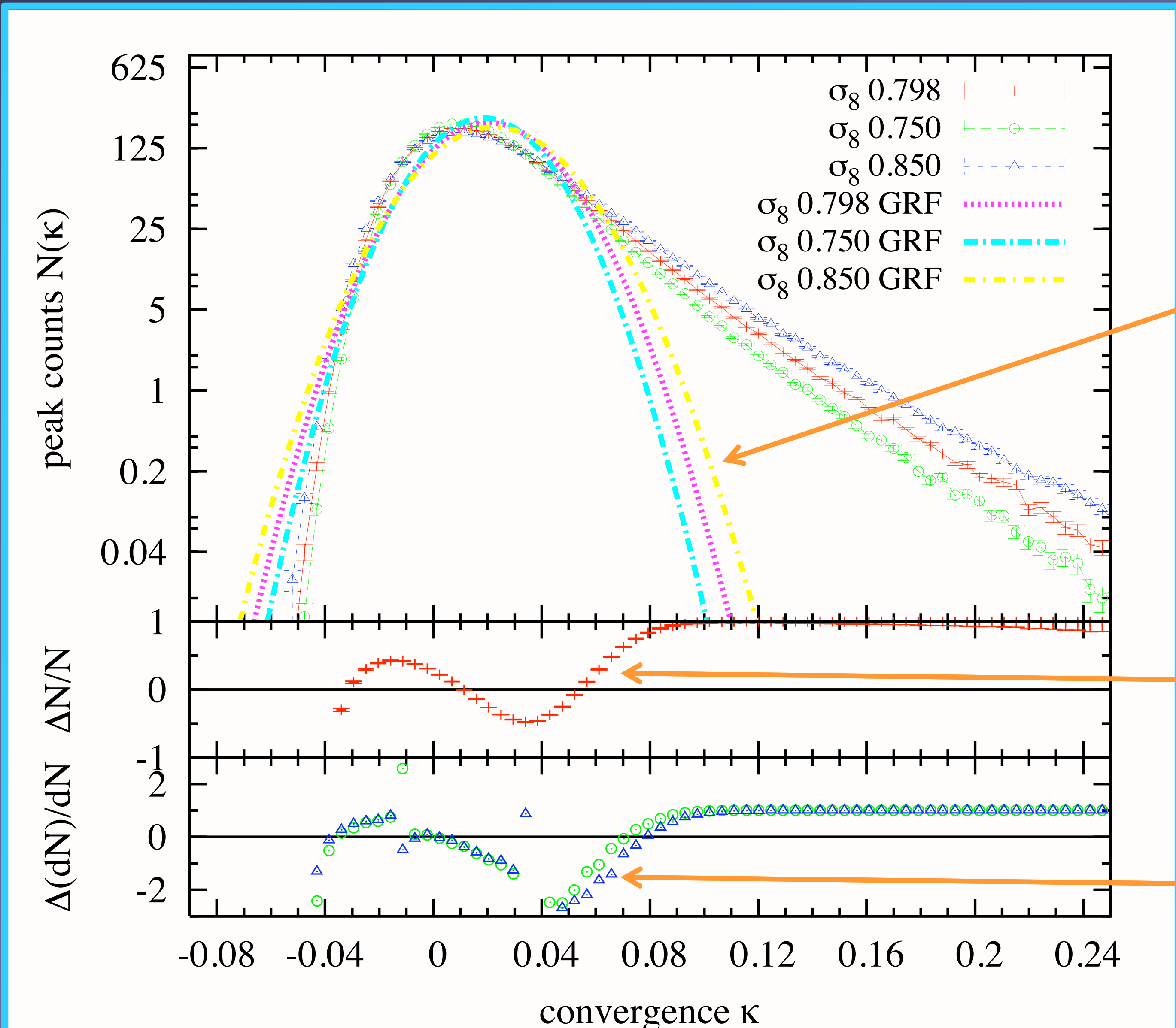

analytic predictions for GRF

Peak counts Non-Gaussian

Cosmology dependence Non-Gaussian

Which peaks dominate constraints?

- high σ_8: more peaks at high+low ends
- low σ_8: peaks are more sharply peaked
- low ($\kappa \approx 0.02$-0.04, or 1-2σ) peaks dominate total χ^2

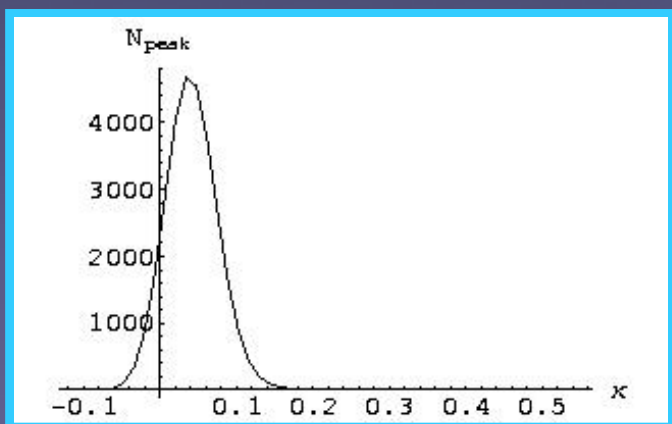

Total # of peaks

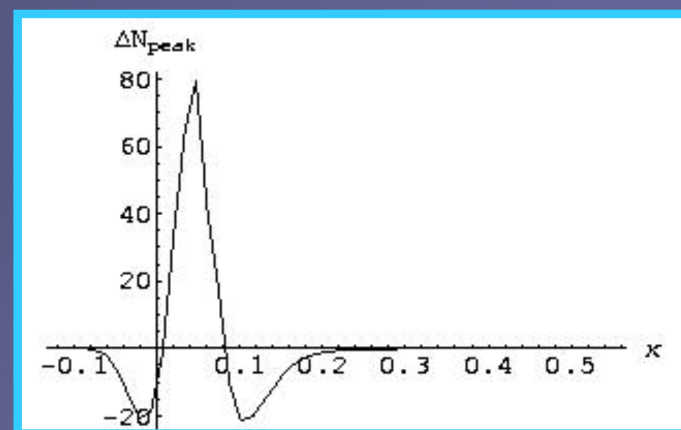

Difference in N_{peak}

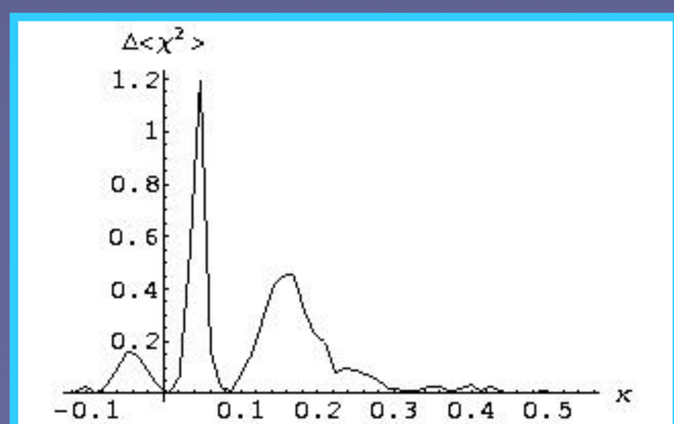

Contribution to χ^2

Origin of Peaks

- **What causes the low peaks?**

  (i) one or more individual collapsed halos
  (ii) mildly over-dense large-scale filaments
  (iii) unvirialized 'half-collapsed' halos
  (iv) galaxy shape noise

  - identify halos, match them to peaks [use fiducial cosmology]:

  only ~10% of low peaks have unique halo match

- **What drives cosmology-dependence of peak counts?**

  - compare two different cosmologies (e.g. vary σ_8) with identical noise realization and (quasi) identical initial condition to match individual peaks in two different cosmologies:

  low peaks 'fragile' – about 50% have a match

What causes peaks?

high peaks | **low peaks**

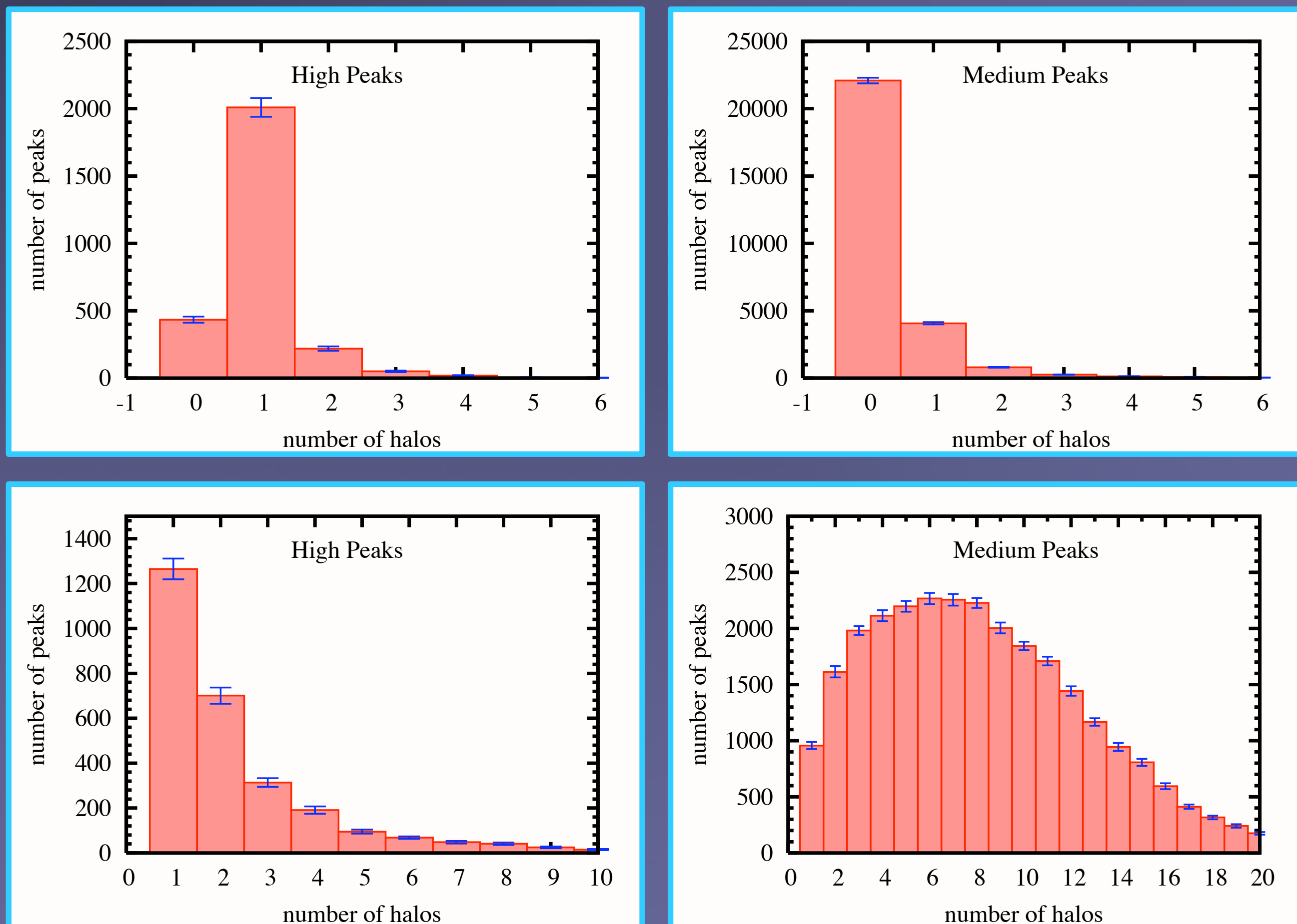

noise or halo contributions

halo only contributions

low peaks are created by *shape noise* + constellation of 4-8 *halos* along the LOS

High vs low peaks

High peaks (S/N>3)
Massive halos

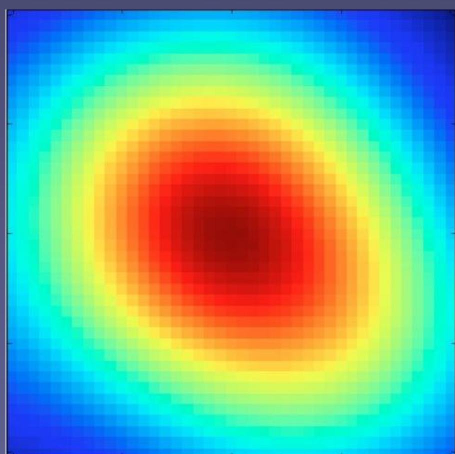

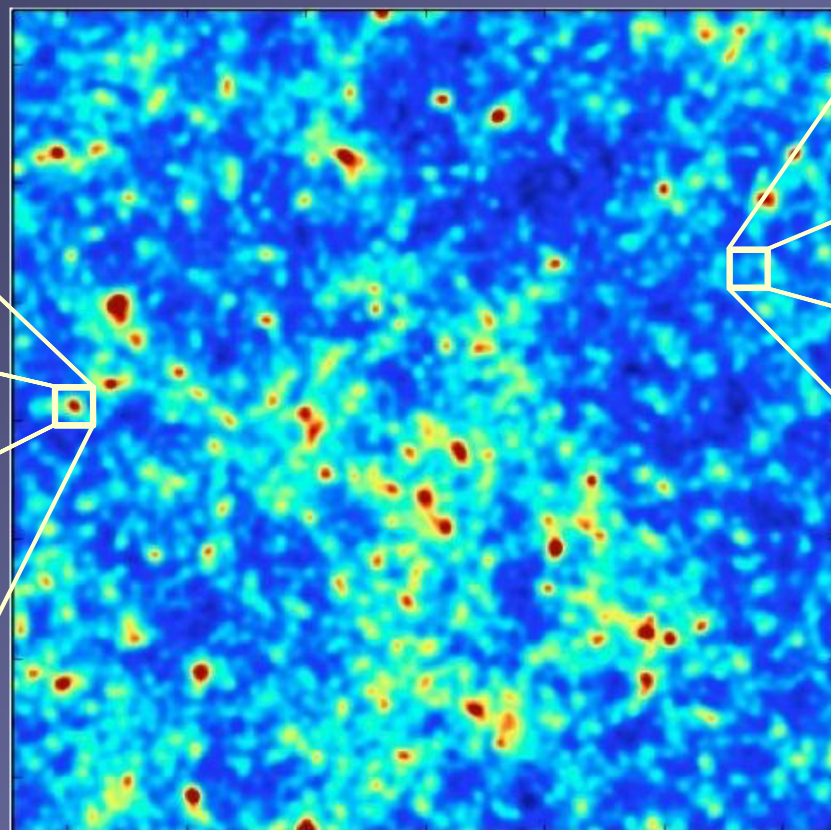

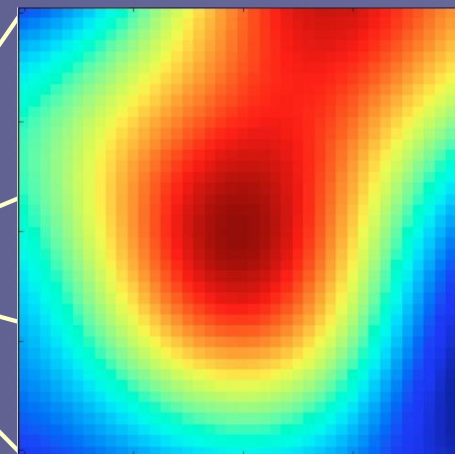

Low peaks (S/N<3)
Constellations of several small halos, or aligned filaments (?)

Outline

- Overview of weak lensing and current results
- Lensing is not Gaussian!
- Cosmology with peak counts
- Application to CFHT data
- Alternative non-Gaussian statistics
- Systematic errors: theoretical + observational

CFHTLenS fields

$154\ \mathrm{deg}^2$, $i_{AB} \leq 24.5$

6 million galaxies

$z_{mean} = 0.37$

$n_{gal} = 10$ gals / amin^2

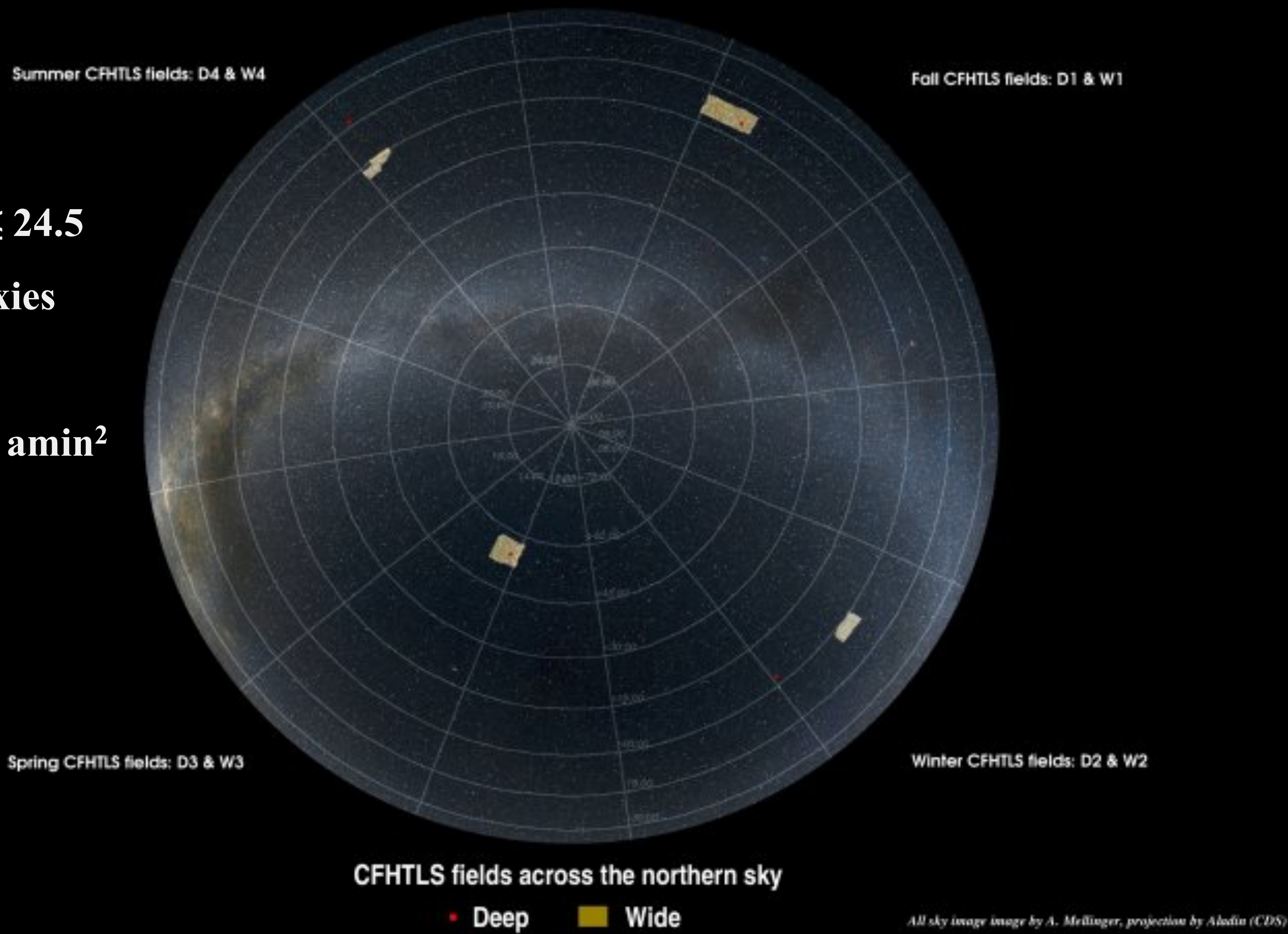

Emulating CFHTLenS

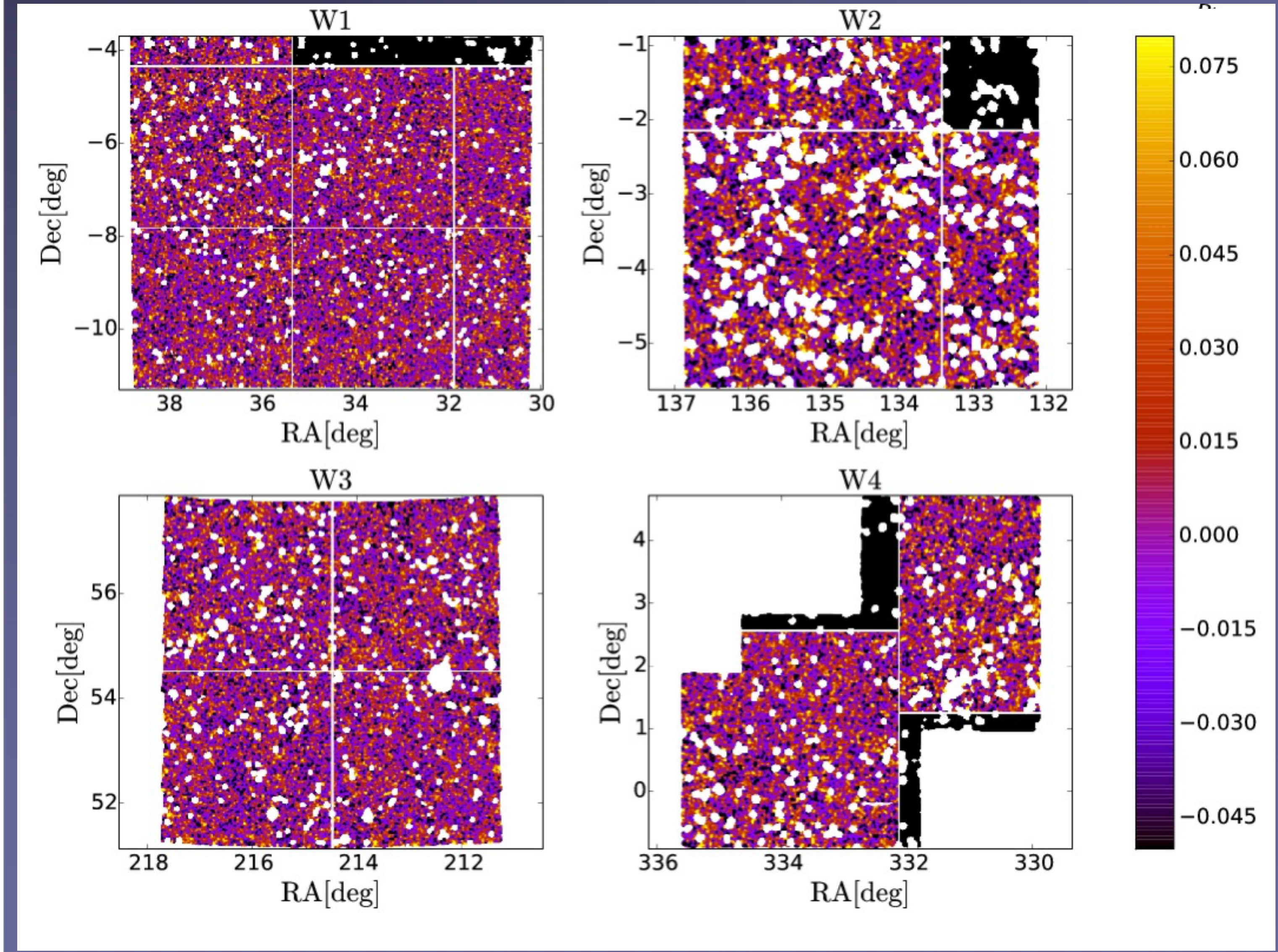

← CFHTLenS convergence maps

Liu et al. 2015

Emulating CFHTLenS

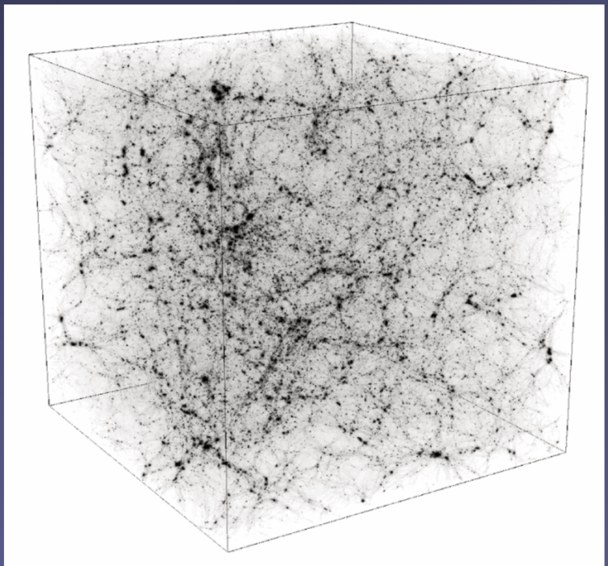

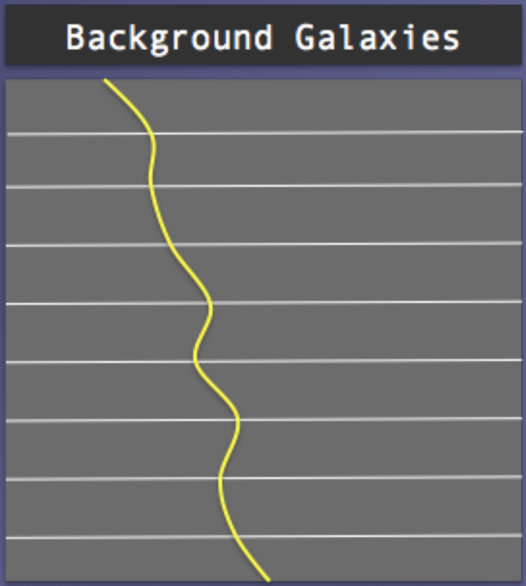

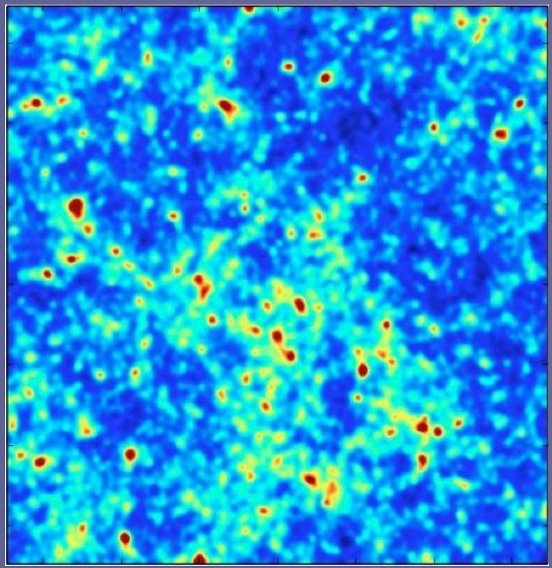

(1) N-body sims (Gadget): 91 cosmological models

(2) Ray-tracing to each of the 6 million galaxies

(3) Convergence maps (1000 realizations/model)

- Tile CFHT fields
- Raytrace to actual $4x10^6$ galaxy positions
- Add random shape noise by random rotations of galaxies
- Create convergence maps
- Repeat in each of the 91 cosmologies (1000 per cosmology)

Emulator: cosmology-dependence

- Irregular grid
- Latin hypercube in 3D
- 91 cosmologies

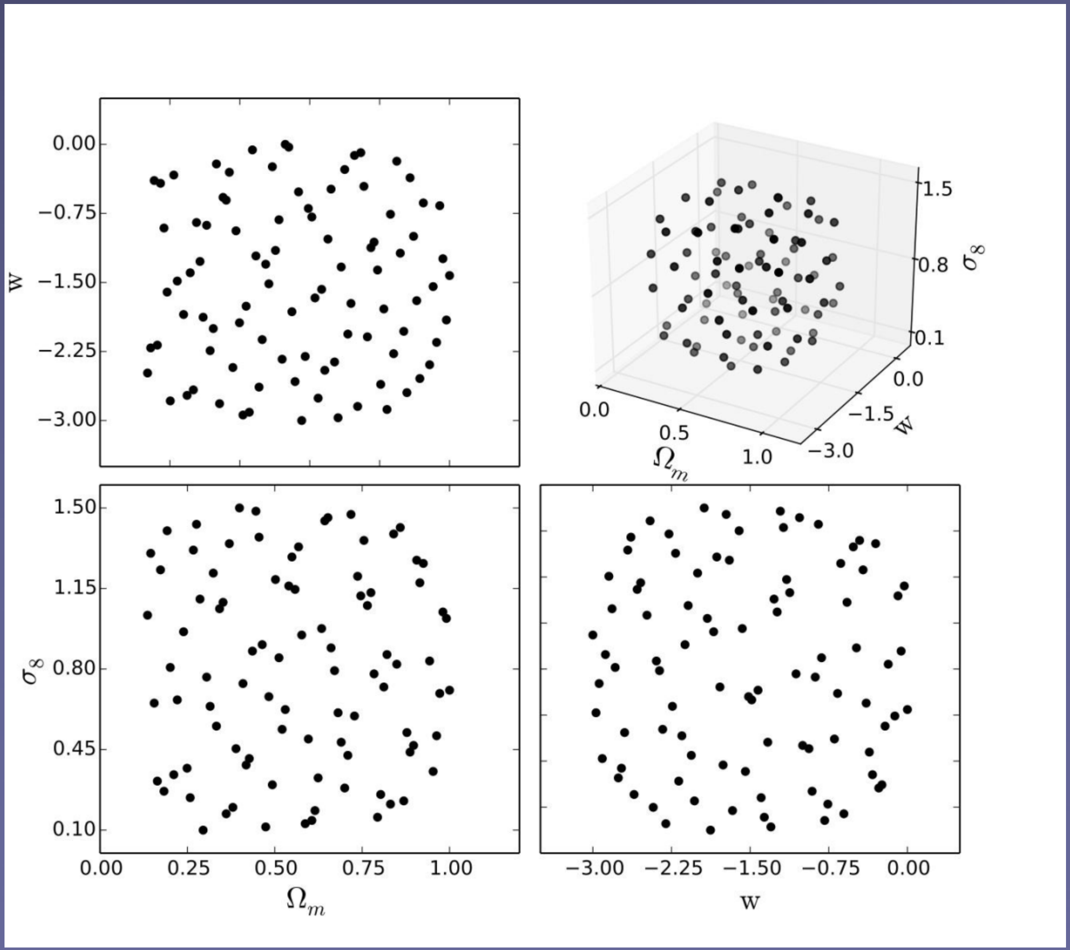

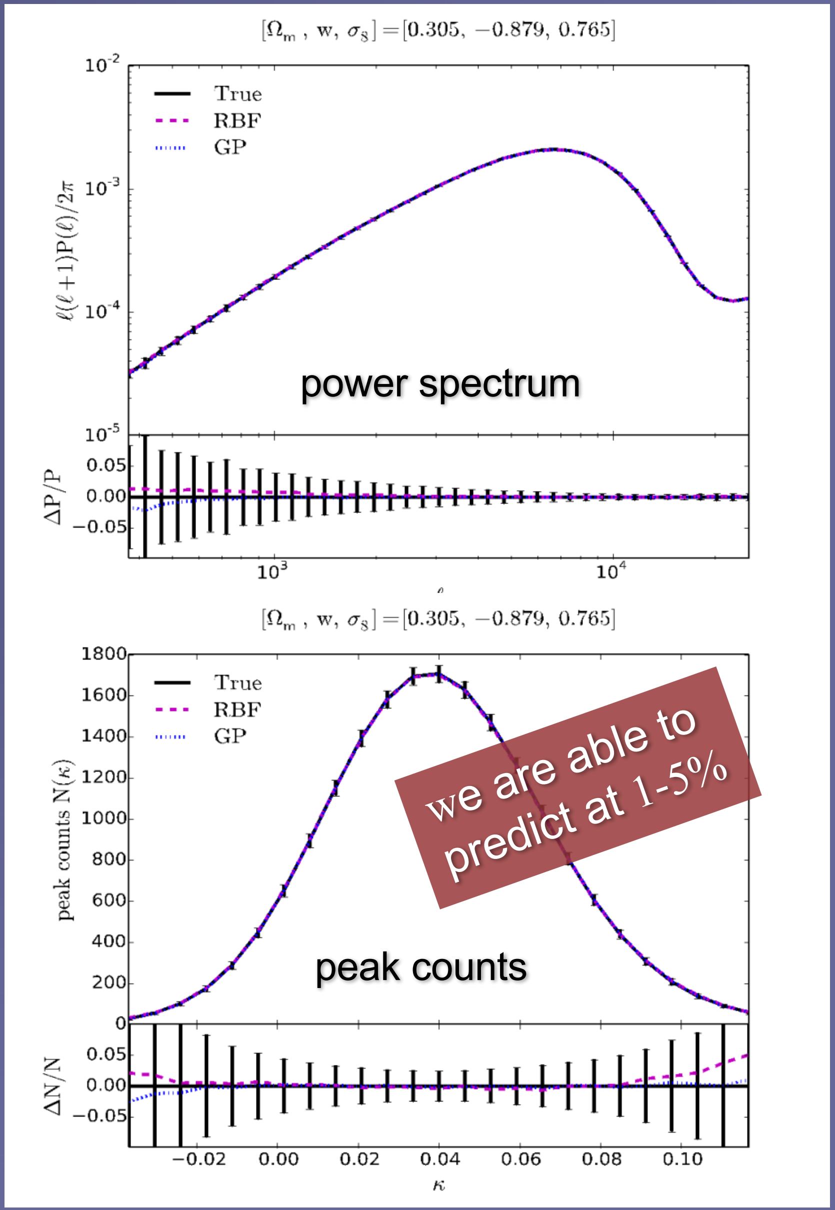

Results

Bayesian confidence levels computed directly (no MCMC)

- **w unconstrained (without tomography)**
- **Adding peaks improves constraint by factor ~2**
  power spectrum not needed
- **Cross-check on systematics**

	w–Ω_m		Ω_m–σ_8	
	68%	95%	68%	95%
power spectrum	1.00	1.74	1.00	1.99
peak counts	0.41	1.01	0.59	1.51
combined	0.42	1.05	0.61	1.46

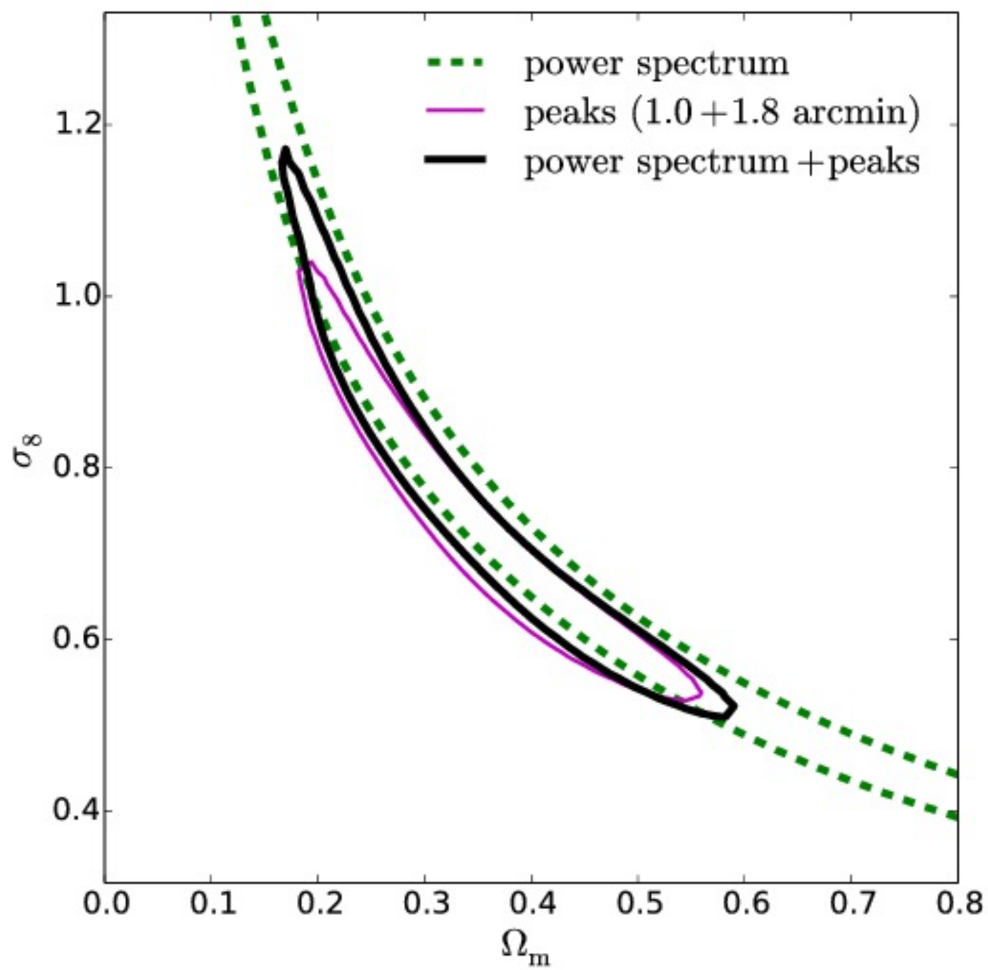

Results: best fits

Power spectrum

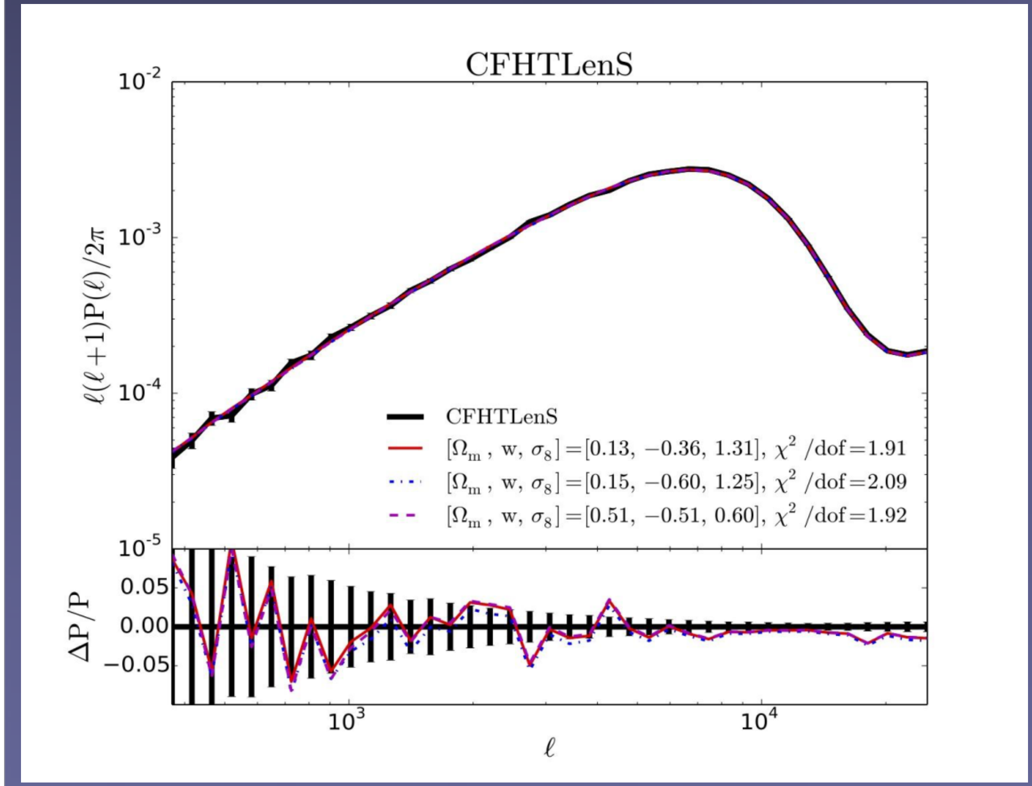

Peak counts

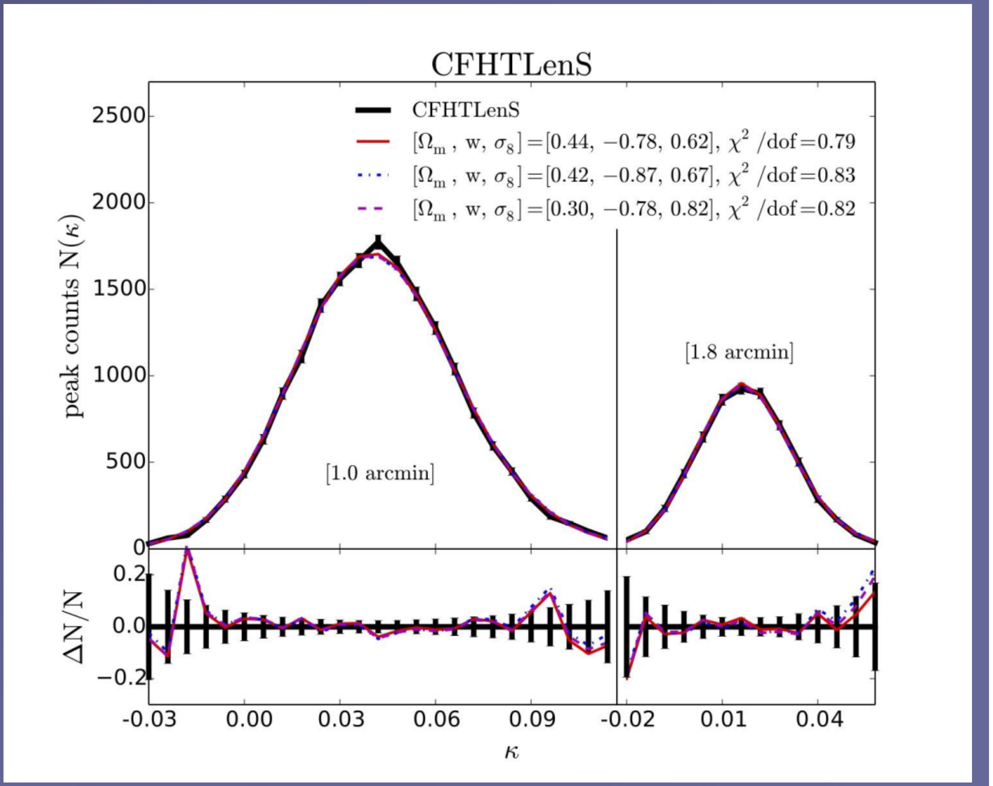

Results on amplitude parameter

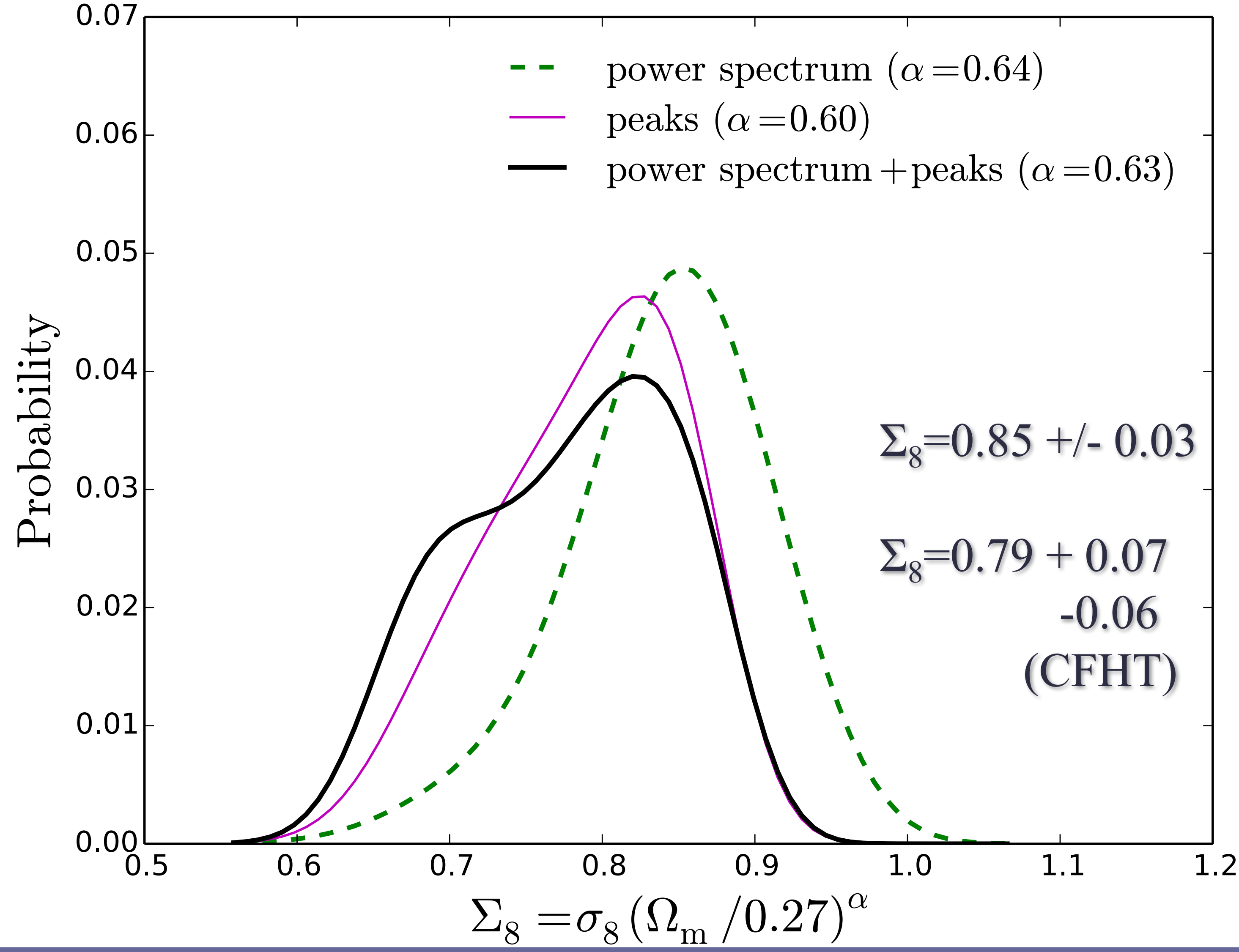

Results: multiple smoothing scales

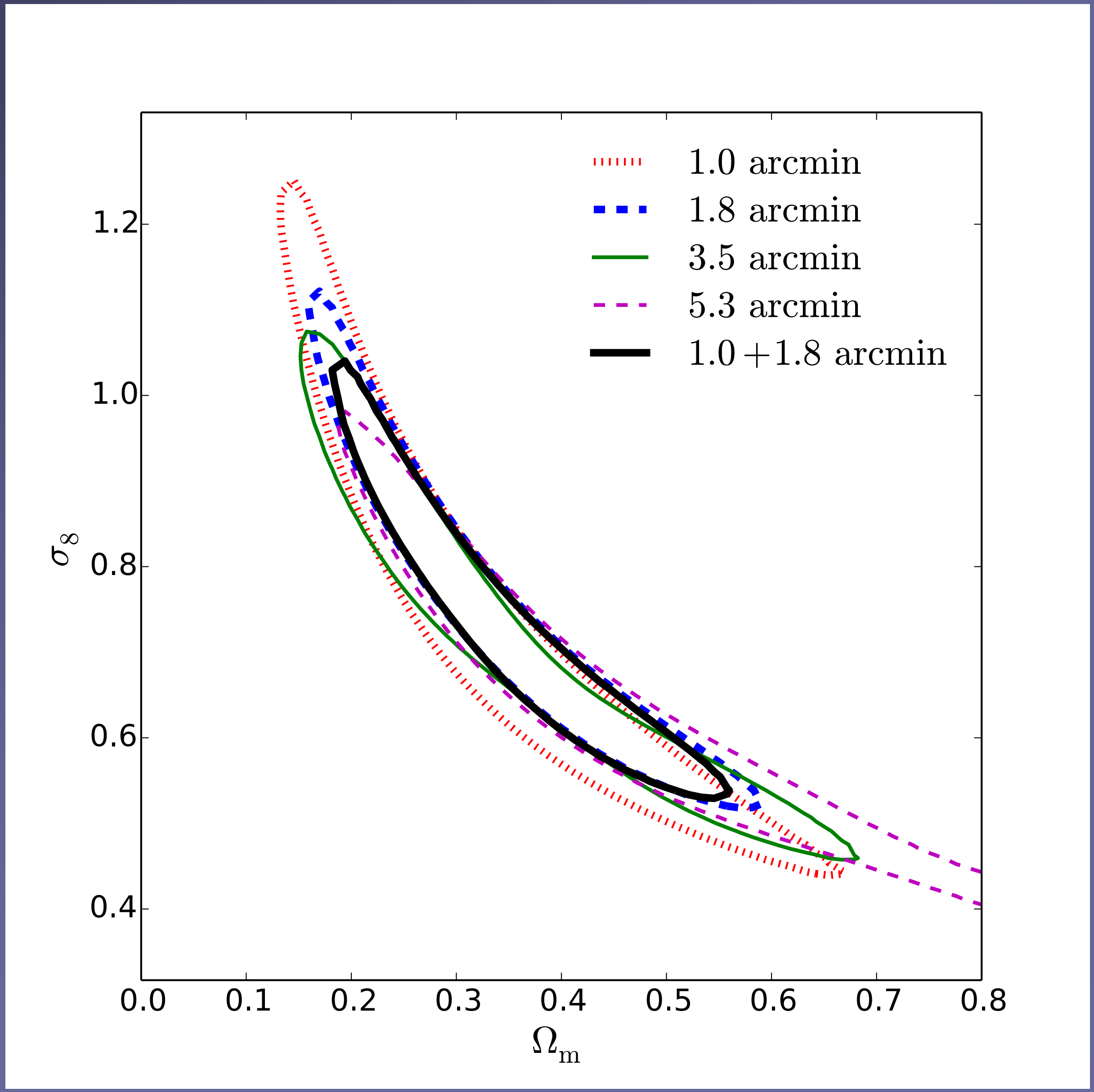

Similar results from recent DES SV

Kacprzak et al. 2016 (arxiv:1603.05040)

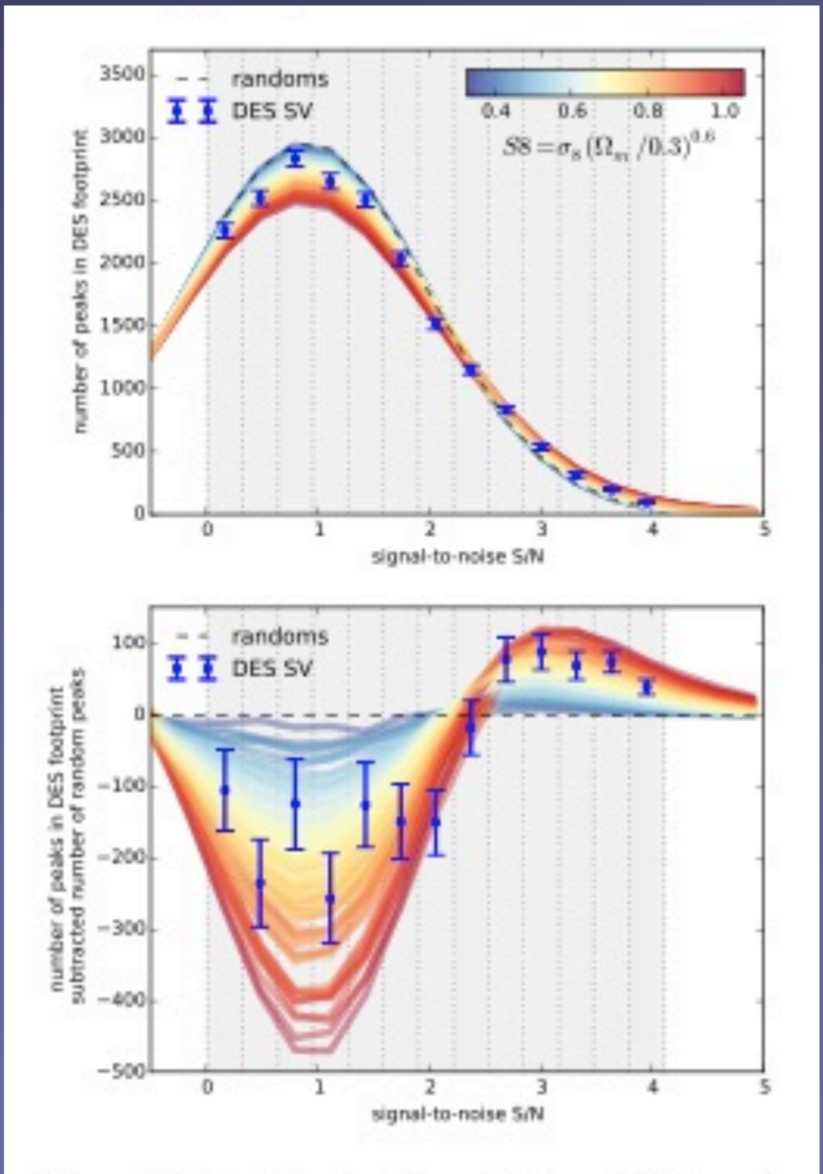

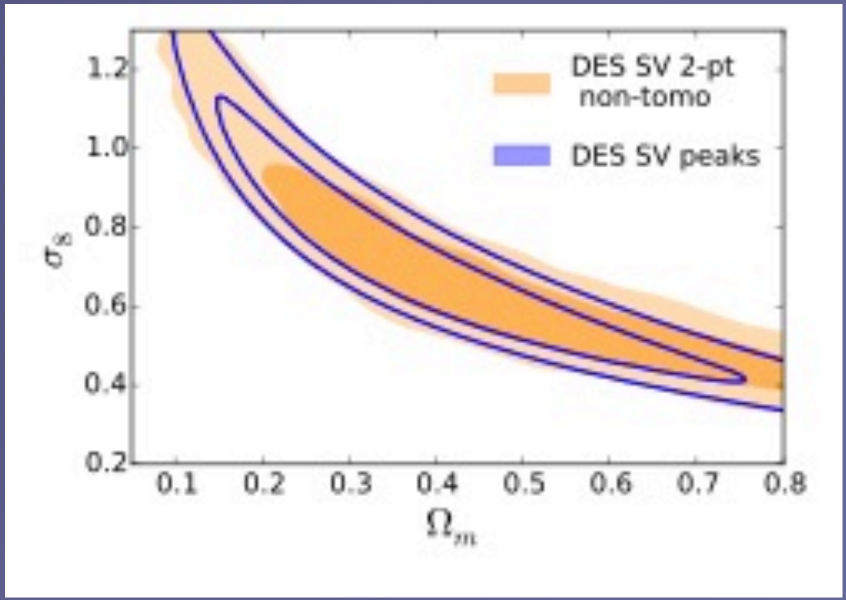

$$\Sigma_8 = \sigma_8(\Omega_m/0.3)^{0.6} = 0.77 +/- 0.07$$

Marginalized over systematics:

- photo-z errors
- intrinsic alignment model
- multiplicative shear bias
- blending, source contamination

Outline

- Overview of weak lensing and current results
- Lensing is not Gaussian!
- Cosmology with peak counts
- Application to CFHT data
- Alternative non-Gaussian statistics
- Systematic errors: theoretical + observational

Results for CFHTLenS

Nine Low-Order Moments (LMs)

$$\mathrm{LM}_2 : \sigma^2_{0,1} = \langle \kappa^2 \rangle, \langle |\nabla \kappa|^2 \rangle,$$

$$\mathrm{LM}_3 : S_{0,1,2} = \langle \kappa^3 \rangle, \langle \kappa |\nabla \kappa|^2 \rangle, \langle \kappa^2 \nabla^2 \kappa \rangle,$$

$$\mathrm{LM}_4 : K_{0,1,2,3} = \langle \kappa^4 \rangle, \langle \kappa^2 |\nabla \kappa|^2 \rangle, \langle \kappa^3 \nabla^2 \kappa \rangle, \langle |\nabla \kappa|^4 \rangle$$

Three Minkowski Functionals (MFs)

$V_0(\nu)$: area above threshold

$V_1(\nu)$: length of boundary

$V_2(\nu)$: # of connected region − # of holes

Results for CFHTLenS

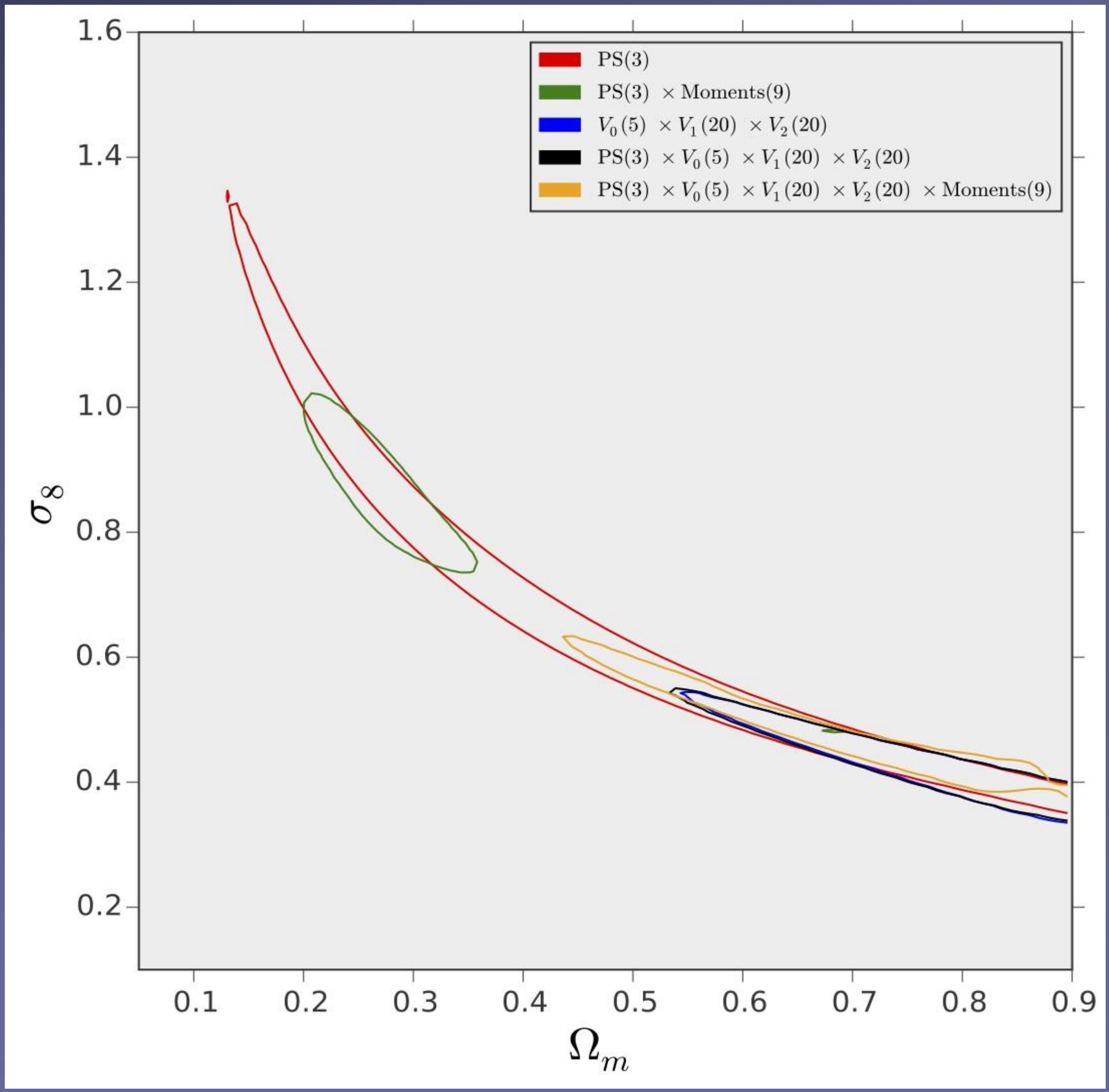

Significant reduction in allowed area from LM

Entirely along degenerate direction

MFs alone are biased

Outline

- Overview of weak lensing and current results
- Lensing is not Gaussian!
- Cosmology with peak counts
- Application to CFHT data
- Alternative non-Gaussian statistics
- Systematic errors: theoretical + observational

Some possible systematic errors

- Theoretical Issues
  - observable: $\kappa \rightarrow g=\gamma/(1-\kappa)$ (reduced shear)
  - explore full cosmological parameter space
  - impact of (g)astrophysics
  - intrinsic alignments
  - selection bias (e.g. magnification/size bias)
  - sufficient number of simulations

- Experimental issues
  - shape measurement errors (PSF, telescope/optical aberrations)
  - atmospheric PSF variations spurious shear correlations
  - photo-z calibration (bias and scatter)

Impact of Baryons on Peak Counts

Above is based on N-body simulations. How do baryons impact the result?

Conventional Method:

Hydro simulations + modeling cooling, star formation and feed back from supernovae and AGN, using (phenomenological) recipes

e.g. Zentner, Rudd & Hu (2008), Semboloni et al (2011)

Alternative Approach:

N-body simulations + modifying the halo density profiles by hand, by increasing concentration c_{NFW}

justification: this mimics very closely the cooling and contraction of baryons in DM halos.

caveat: does not capture AGN feedback

The Impact of Baryons

Change in power spectrum and peak counts, by 50% increase concentration parameter

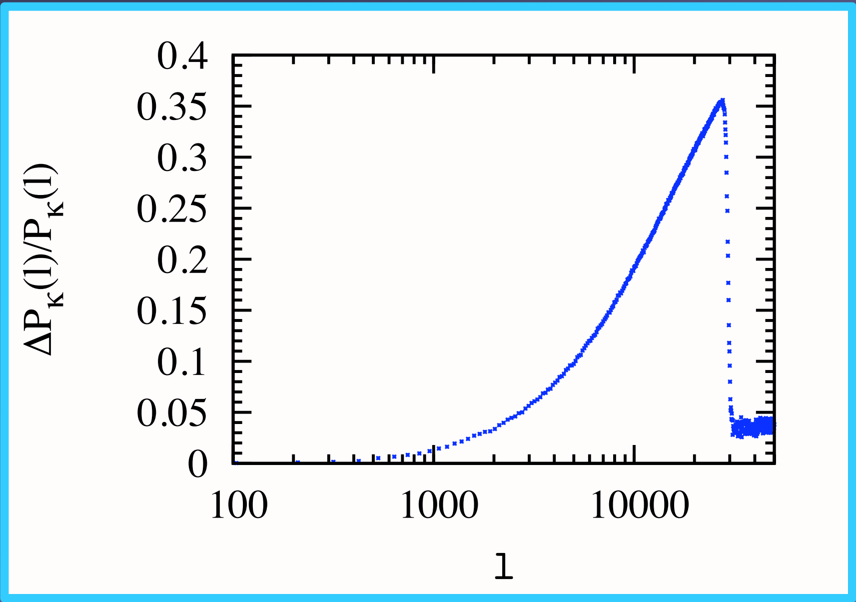

power spectrum:

increase on small scales.
results agree with Zentner et al. (2008)

(sharp drop at l=20,000 is due to 1 arcmin smoothing.)

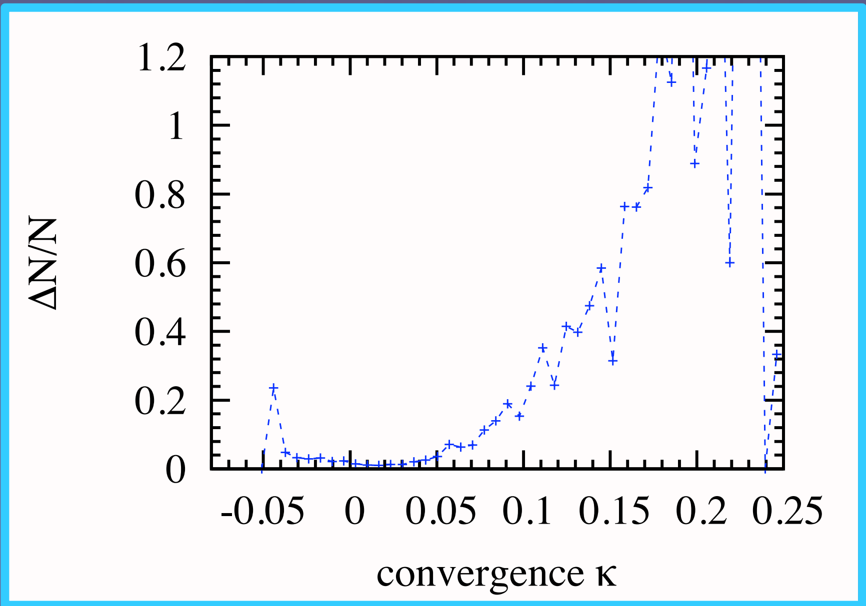

peak counts:

- strong increase in # of high peaks
- very little change in # of low peaks

A promising result!
low peaks contain most of cosmology info – don't need high peaks.

cf: most of the constraints are lost if power spectrum at l>1000 is ignored

Why Are Low Peaks Robust ?

halos contributing to low peaks have lower mass ($10^{12} – 10^{13}\ M_{\odot}$ vs. $10^{14}\ M_{\odot}$ for high peaks) and larger off-set from the line-of-sight towards each peak

Distribution of impact parameters *d/R_{vir}*

0 - 0.2 (high peaks)

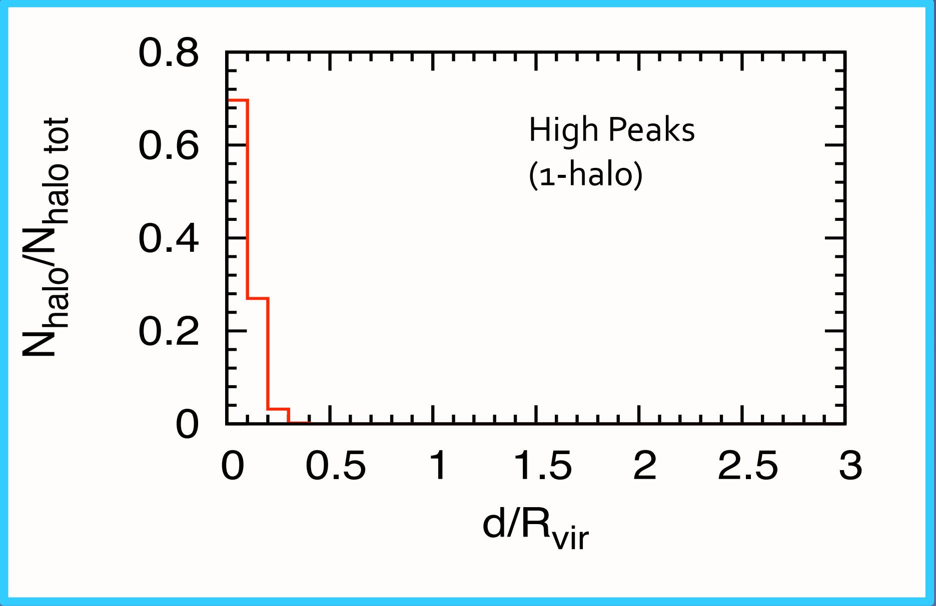

0.5 - 0.9 (low peaks)

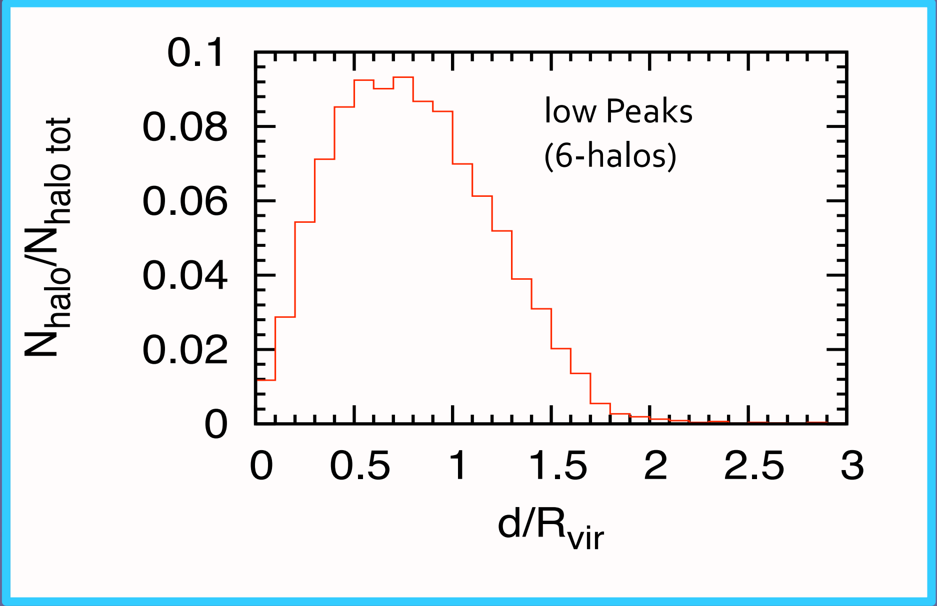

Bias in Inferred Cosmology

Peak counts

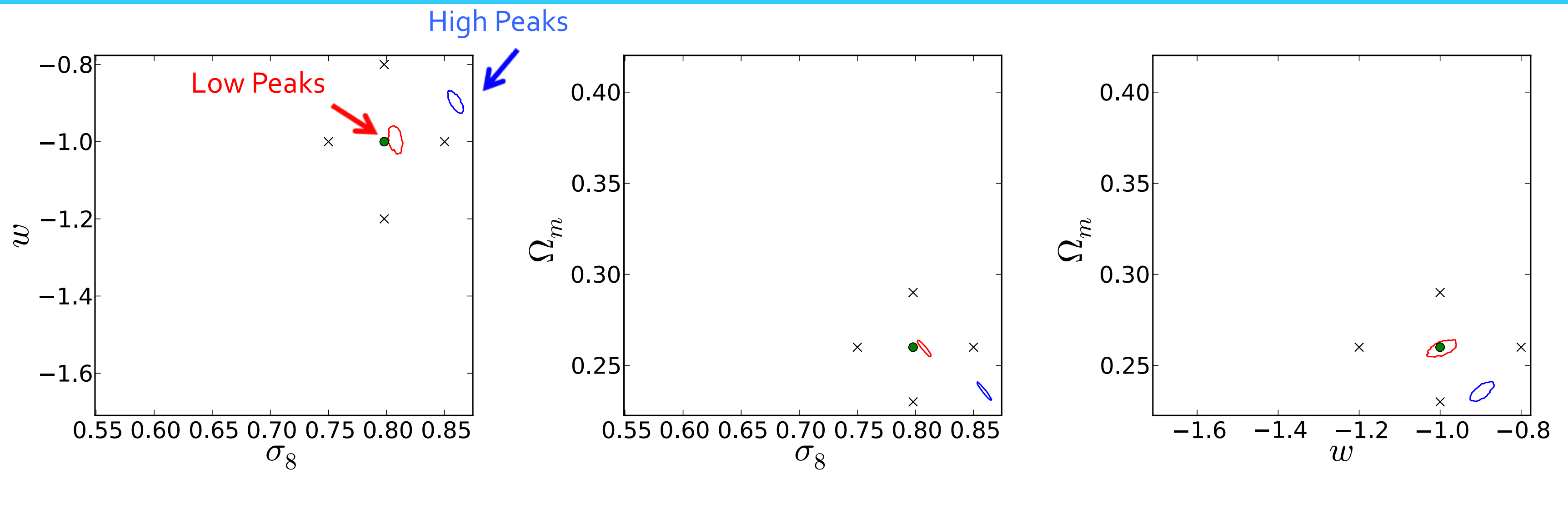

Power spectrum

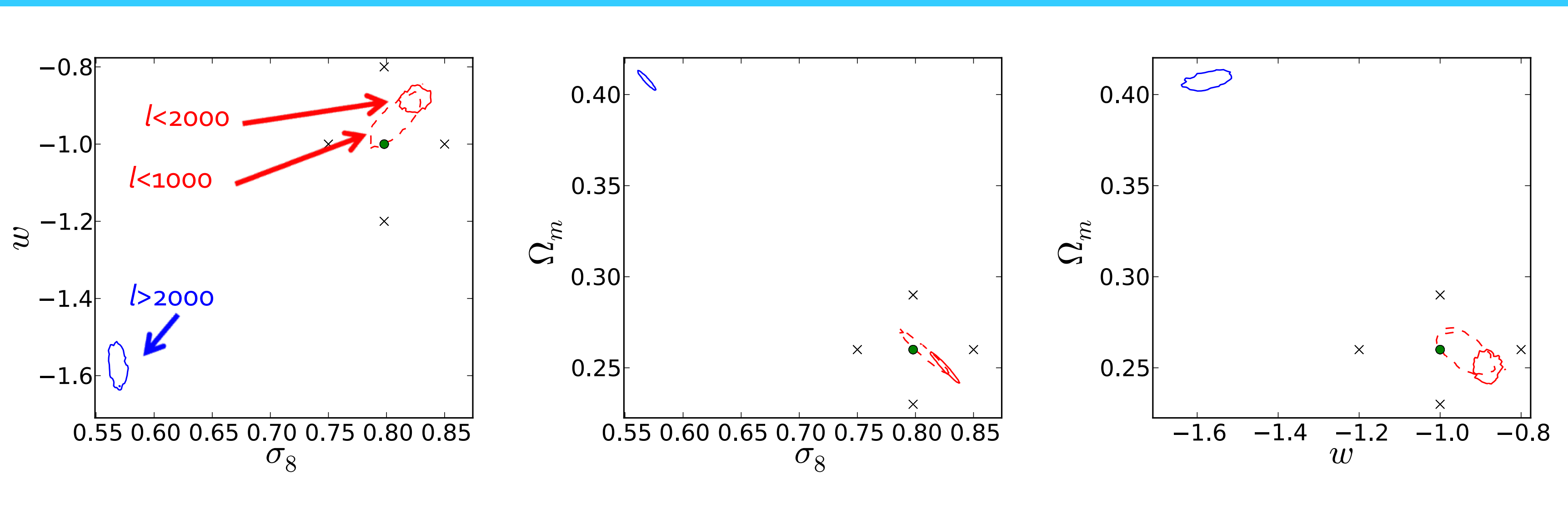

Conclusions

- Theory: Peaks, MFs, and moments constrain Ω_m, w, σ_8 comparable or tighter than the power spectrum – errors improve by factors of 2-3.

- This information is new: arises from non-linear, non-Gaussian regime, and is beyond the power spectrum

- Peaks: most info is in low (1-2σ) peaks, from projections of 4-8 halos appear to be robust to baryonic effects – allow self-calibration

- Fits to CFHTLenS data: predictions confirmed! Peaks and quartic moments offer factor of two improvement on Ω_m-σ_8 constraints

The End